Supporting Information for

Multi-colour and red emissions from a small donor-acceptor molecule by breaching Kasha's rule

Prathaban G,[a] Akanksha Sharma,[b] Soumen De,[b] and Susnata Pramanik*[a]

[a]Faculty of Engineering and Technology, Department of Chemistry, SRM Institution of Science and Technology (SRMIST), Kattankulathur 603203, India.gmail : susmatap@srmist.edu.in

[b]School of Chemistry, Indian Institute of Science Education and Research (IISER), Thiruvananthapuram, Kerala 695551, India.

Table of contents

1. General remarks 3

2. Synthetic methods 3

2.1 Synthetic procedure for 5-Nitro acenaphthaquinone 3

2.2 Synthetic procedure for 5-Methoxy acenaphthoquinone 4

2.3 Synthetic procedure for Compound 1 4

2.4 Synthetic procedure for Compound 2 5

2.5 Synthetic procedure for Compound 3 6

3. NMR & HRMS Characterization 7

4. HPLC Analysis 10

5. Photophysical studies 12

6. Lifetime measurements 23

7. Quantum yield Measurements: 24

8. Crystallographic Information 31

9. DFT Calculation 35

9.1 Compound 1 Gaussian optimization 36

9.2 Compound 2 Gaussian optimization 40

9.3 Compound 3 Gaussian optimization 45

1. General remarks

All glassware is cleaned and dried before use. Chemicals were purchased from TCL, Avra, and SRL and utilized without further purification. Thin-layer chromatography was performed on TLC Silica gel 60 F_{254} (2x4 cm). Silica gel (100-200 mesh) was used for column chromatography. NMR Bruker Avance Neo (500 MHz) spectrometer was used to record the NMR spectra. ^{1}H NMR (500MHz) and ^{13}C NMR (101 MHz) chemical shifts were measured relative to $SiMe_4$ and $CDCl_3$, using the chemical shift of the residual solvent peaks as references ($SiMe_4$: δ 0 ppm). In NMR, the signal multiplicities are denoted by the letters s, d, m, dd, and t, which stand for singlet, doublet, multiplet, doublet of doublet, and triplet, respectively. High-resolution mass spectra (HR-MS) were recorded using an Agilent Technologies 6230 Q-TOF LC/MS system with Electrospray Ionization (ESI). HPLC data were collected in an Agilent 1260 Infinity HPLC using pure acetonitrile as eluent and C-18 column. UV analysis was performed on Carry 60 UV-Vis instrument from Agilent using HPLC grade solvents. Fluorescence spectra were recorded in Edinburg Instruments FLS 1000. The fluorescence decay curve and quantum yield were collected on the Edinburg Instruments FLS 1000 spectrofluorometer. Single crystal X-ray diffraction analysis was done using a Bruker D8 Quest X-ray diffractometer with Mo Kα (λ = 0.71073 Å) radiation. All theoretical calculations were performed using Gaussian 16, Revision A.03. The time-dependent density functional theory (TDDFT) calculations of the excitation energies were calculated at the optimized geometries of the ground states.

2. Synthetic methods

2.1 Synthetic procedure for 5-Nitro acenaphthaquinone[i]

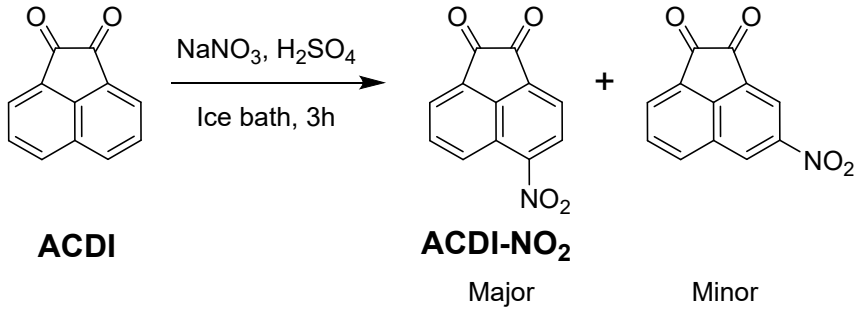

Scheme S1. Synthetic scheme of 5-Nitroacenaphthaquinone.

Acenaphthoquinone (1.00 g, 5.48 mmol), and $NaNO_3$ (513 mg, 6.03 mmol), were taken in RB flask and placed in an ice bath. Conc. H_2SO_4 (10 mL) was slowly added with constant stirring. After the addition, the reaction is stirred for 3 h at room temperature. Then, the reaction mixture was slowly transferred into crushed ice. The formed precipitates were filtered and washed with water and purified by column chromatography using Ethyl acetate/hexane (30%:70%, v/v) as the eluent. Subsequently, recrystallized from dichloromethane. Yellow needle-like crystals were obtained (60% yield).

2.2 Synthetic procedure for 5-Methoxy acenaphthoquinone[i]

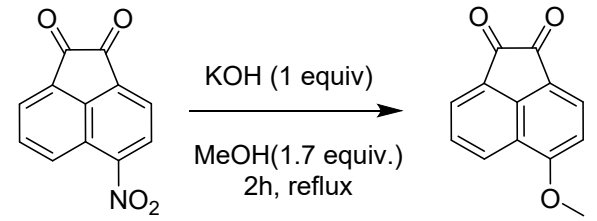

Scheme S2. Synthetic scheme of 5- Methoxy acenaphthoquinone.

5-Nitroacenaphthoquinone (300 mg, 1 equiv., 1.32 mmol), KOH (75 mg, 1 equiv., 1.32 mmol), were dissolved in 10 mL of Methanol and refluxed for 2 h. The solvent was removed, and the crude product was purified by column chromatography using Ethyl acetate/hexane (50%:50%, v/v) as the eluent. Light yellow powder obtained (60% yield).

2.3 Synthetic procedure for Compound **1**

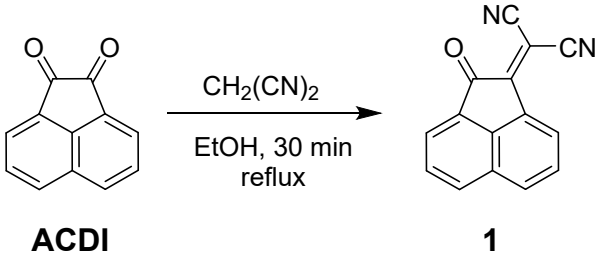

Scheme S3. Synthetic scheme of Compound **1**

Acenaphthoquinone (300 mg, 1 equiv., 1.64 mmol) and malononitrile (152 mg, 1.2 equiv., 1.97 mmol) were dissolved in 10 mL of ethanol and refluxed for 30 minutes. The obtained precipitate was filtered and washed with cold ethanol and recrystallized from dichloromethane. Red plate crystals obtained.

Yield: 85%. Melting point: 232-238 °C. ^{1}H NMR (500 MHz, 298 K, $CDCl_3$) δ 8.59 (d, J = 7.5 Hz, 1H), 8.26 (dd, J = 2.0 Hz, J = 8.5 Hz, 2H), 8.18 (d, J = 7.0 Hz, 1H), 7.90 – 7.86 (m, 2H). ^{13}C NMR (126 MHz, 298 K, $CDCl_3$) δ 185.9, 155.3, 142.9, 132.5, 132.3, 130.6, 129.3, 129.2, 129.1, 128.4, 124.6, 123.8, 112.6, 110.8, 81.7. ESI-HRMS: m/z (%): 231.0549 ($[C_{15}H_6N_2O•H]^+$), calcd. m/z = 231.0553. Elemental analysis: C: 78.26; H: 2.63; N: 12.17 found C: 78.22; H: 2.56; N: 12.09.

2.4 Synthetic procedure for Compound **2**

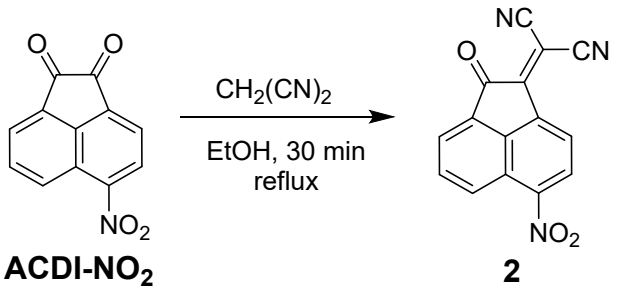

ACDI-NO_2 **2**

Scheme S4. Synthetic scheme of Compound **2.**

5-Nitroacenaphthoquinone (300 mg, 1.32 mmol), and malononitrile (175 mg, 2.64 mmol) were dissolved in 10 mL of ethanol, and refluxed for 30 minutes. The obtained precipitates were filtered, washed in cold ethanol, and dried. Yellow powder obtained.

Yield: 82%. Melting point: 241-255 °C. ^{1}H NMR (500 MHz, 298 K, $CDCl_3$) δ 9.14 (d, J = 8.0 Hz, 1H), 8.76 (d, J = 8.0 Hz, 1H), 8.71 (d, J = 8.0 Hz, 1H), 8.35 (d, J = 7.0 Hz, 1H), 8.18 (t, J = 8.0 Hz, 1H). ESI-HRMS: m/z (%): 275.0336 ($[C_{15}H_5N_3O_3]^-$), calcd. m/z = 275.0331. Elemental analysis: C: 65.46; H: 1.83; N: 15.27 found C: 65.31; H: 1.78; N: 15.25.^{13}C cannot be measured due to poor solubility.

2.5 Synthetic procedure for Compound **3**

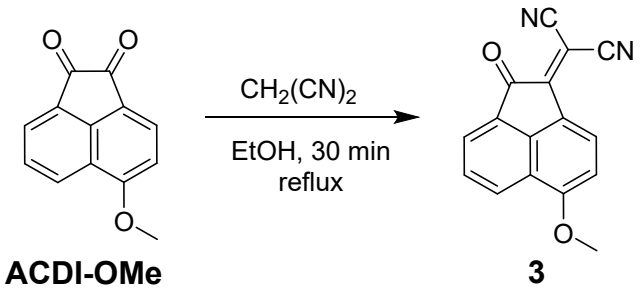

Scheme S5. Synthetic scheme of compound **3**.

5-Methoxy acenaphthoquinone (300 mg, 1.41 mmol) and malononitrile (186 mg, 2.83 mmol) were dissolved in 10 mL ethanol and refluxed for 30 minutes. The obtained precipitate was filtered and washed with cold ethanol, purified by column chromatography using ethyl acetate/hexane (30%:70%, v/v) as the eluent, and recrystallized from ethyl acetate. Reddish brown crystals were obtained.

Yield: 30%. Melting point: 236-245 °C. ^{1}H NMR (500 MHz, 298 K, $CDCl_3$) δ 8.57 (d, J = 8.5 Hz, 1H), 8.41 (d, J = 8.5 Hz, 1H), 8.13 (d, J = 7.5 Hz, 1H), 7.80 (t, J = 7.5 Hz, 7.14 (d, J = 8.5 Hz, 1H), 4.20 (s, 3H). ESI-HRMS: m/z (%): 261.0659 ($[C_{16}H_8N_2O_2•H]^+$), calcd. m/z = 261.0654. Elemental analysis: C: 73.84; H: 3.10; N: 10.76 found C: 73.79; H: 3.10; N: 10.75. ^{13}C cannot be measured due to poor solubility.

Please note that the range of melting points for compounds **2** and **3** is high. We observed isomeric impurity (2.4%) in compound **2** which was not possible to isolate due to similar polarity. The presence of impurity can lead to such a high range in melting points. However, we did not observe any impurity in **3**. Therefore, the observed range can be attributed to the highly amorphous nature of compound **3**.

3. NMR & HRMS Characterization

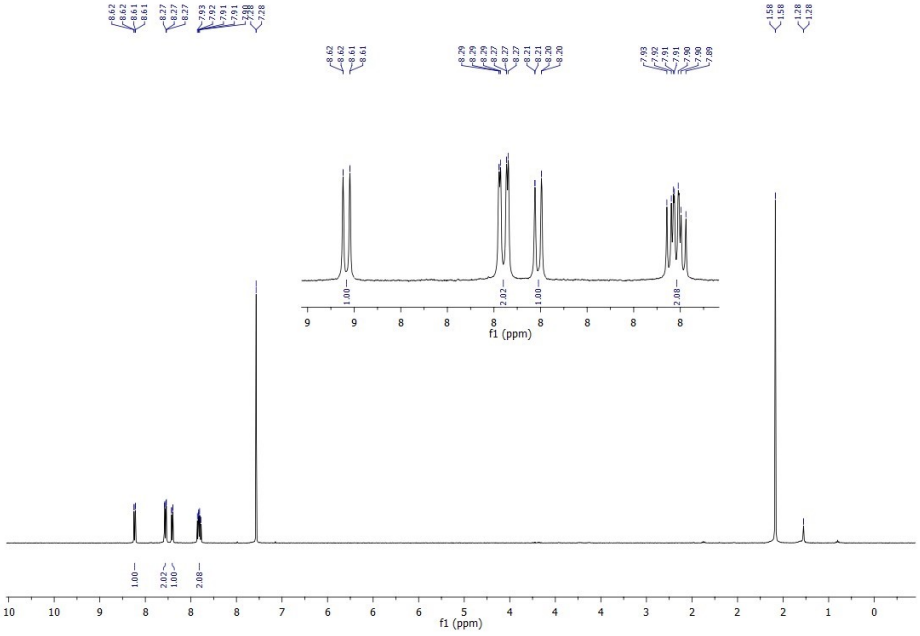

Figure S1. ^{1}H NMR (500 MHz, $CDCl_3$, 298 K) spectrum of compound **1**. The inset shows the zoomed-in version of the aromatic region.

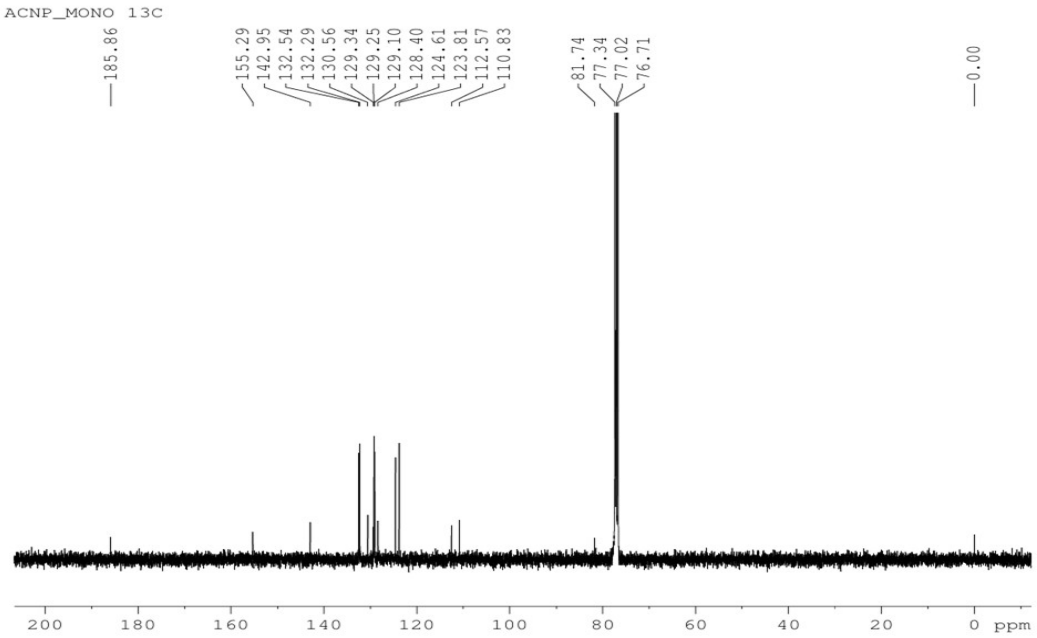

Figure S2. ^{13}C NMR (126 MHz, $CDCl_3$, 298 K) spectrum of compound **1**.

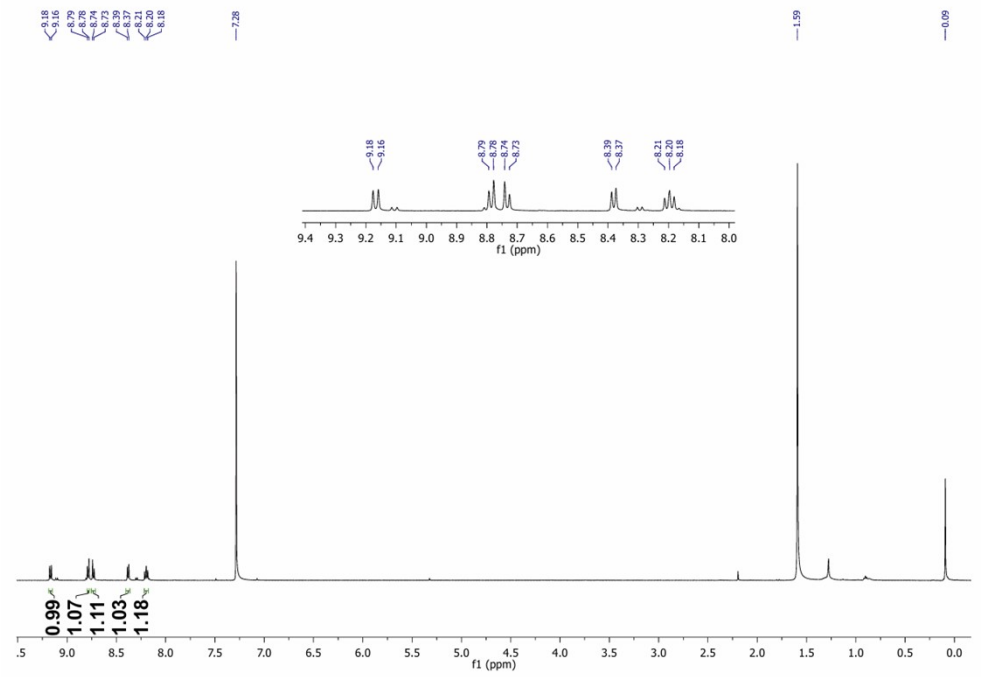

Figure S3. ^{1}H NMR (500 MHz, $CDCl_3$, 298 K) spectrum of compound **2**. The inset shows the zoomed-in version of the aromatic region.

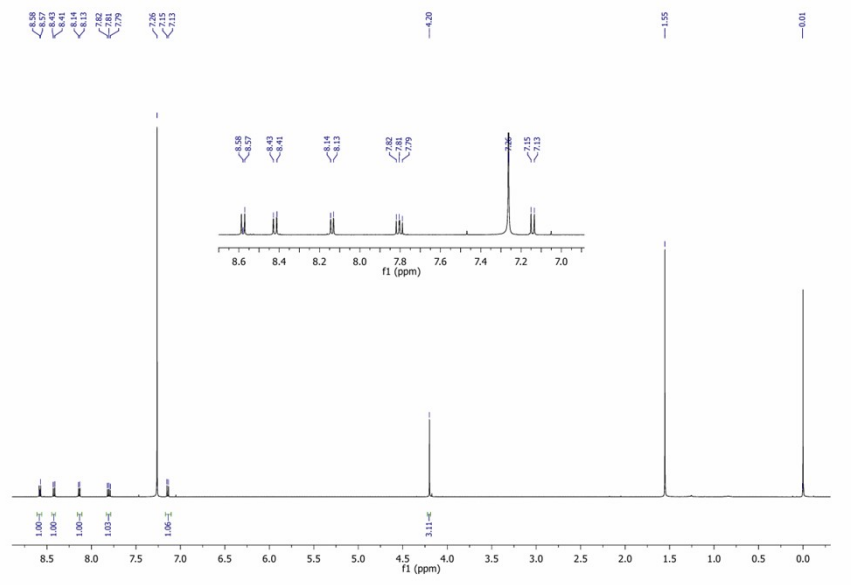

Figure S4. ^{1}H NMR (500 MHz, $CDCl_3$, 298 K) spectrum of compound **3**. The inset shows the zoomed-in version of the aromatic region.

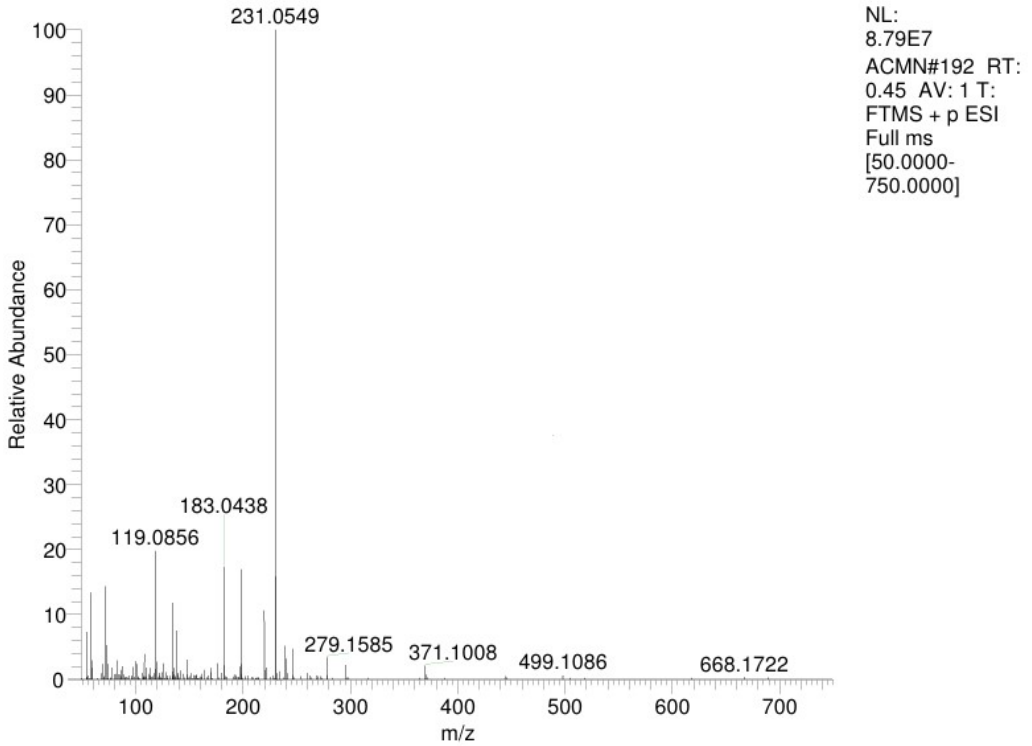

Figure S5. ESI-HRMS spectrum of compound **1**.

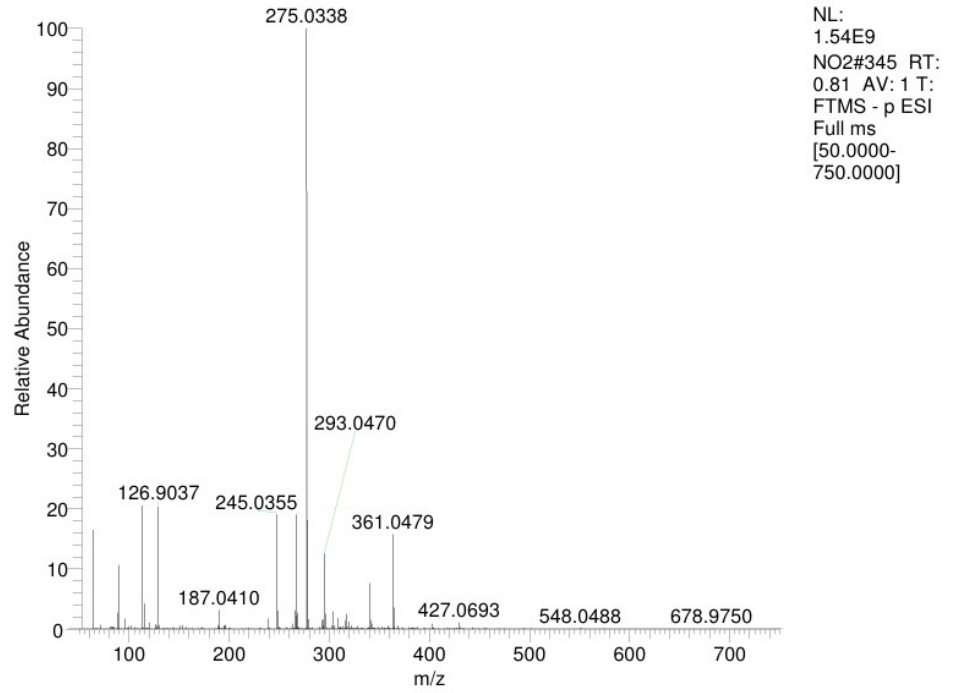

Figure S6. ESI-HRMS spectrum of compound **2**.

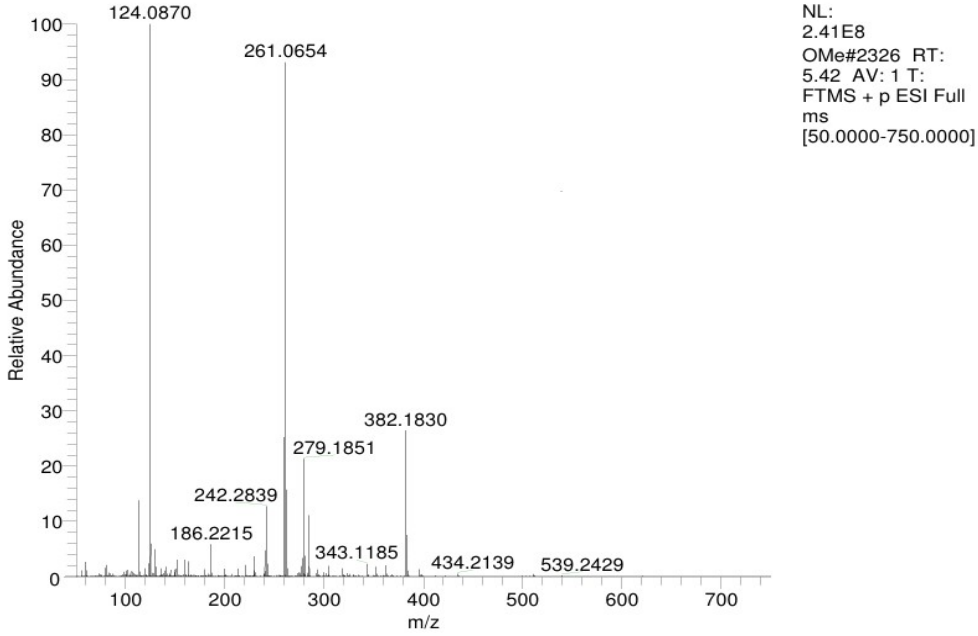

Figure S7. ESI-HRMS spectrum of compound **3**.

4. HPLC Analysis

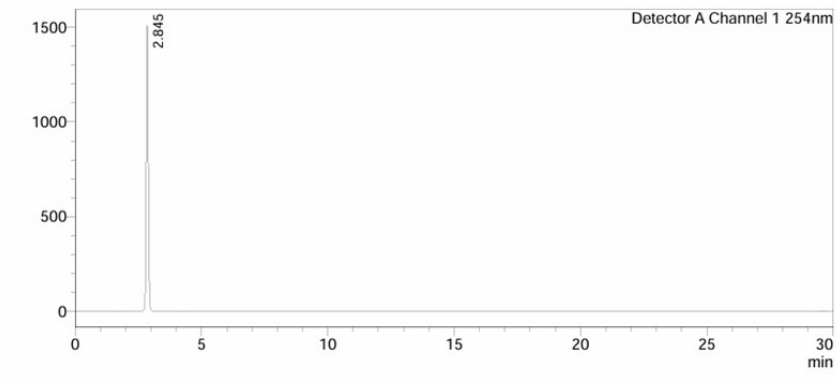

Detector A Channel 1 254nm

Ret. Time	Area	Height	Area%
2.845	8452140	1508582	100.000
	8452140	1508582	100.000

Figure S8. Reverse-phase HPLC chromatogram of compound **1** using acetonitrile as the mobile phase. (HPLC condition: CH_3CN, 30 min, flow rate = 1.0 mL/min, wavelength = 254 nm).

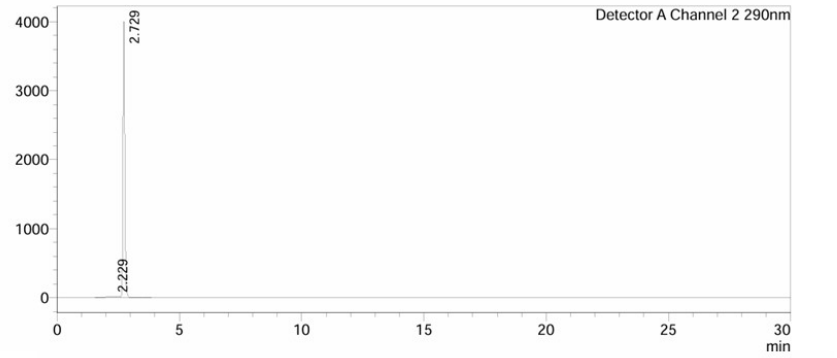

Detector A Channel 2 290nm

Ret. Time	Area	Height	Area%
2.229	497453	18394	2.444
2.729	19853123	3999958	97.556
	20350576	4018352	100.000

Figure S9. Reverse-phase HPLC chromatogram of compound **2** using acetonitrile as the mobile phase. Roughly 2.4% impurity is possibly the other isomer of **2** under HPLC conditions. (HPLC condition: CH_3CN, 30 min, flow rate = 1.0 mL/min, wavelength = 290 nm).

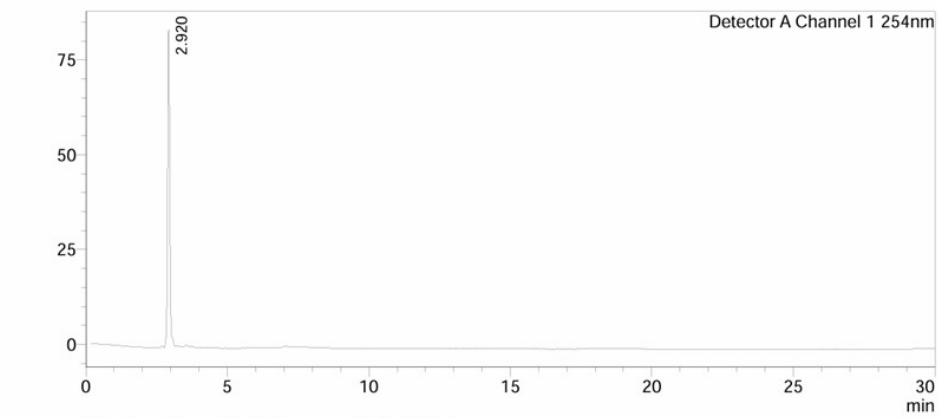

Detector A Channel 1 254nm

Ret. Time	Area	Height	Area%
2.920	447822	83971	100.000
	447822	83971	100.000

Figure S10. Reverse-phase HPLC chromatogram of compound **3** using acetonitrile as the mobile phase. (HPLC condition: CH_3CN, 30 min, flow rate = 1.0 mL/min, wavelength = 254 nm).

5. Photophysical studies

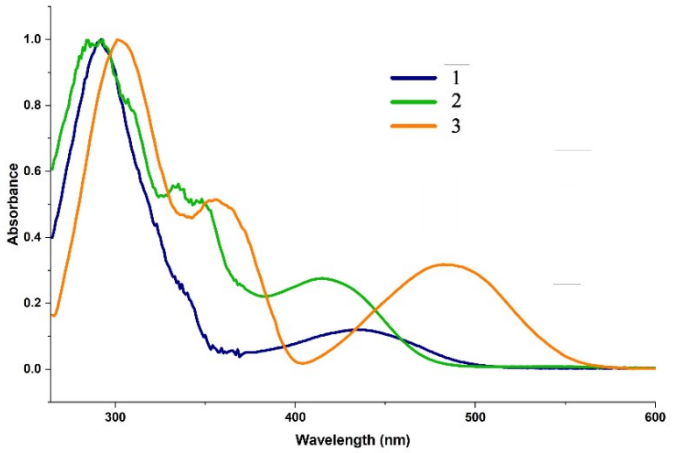

Figure S11. Normalized absorption spectra of compounds **1-3** in CH_3CN ($c = 10^{-5}$ M, 298 K).

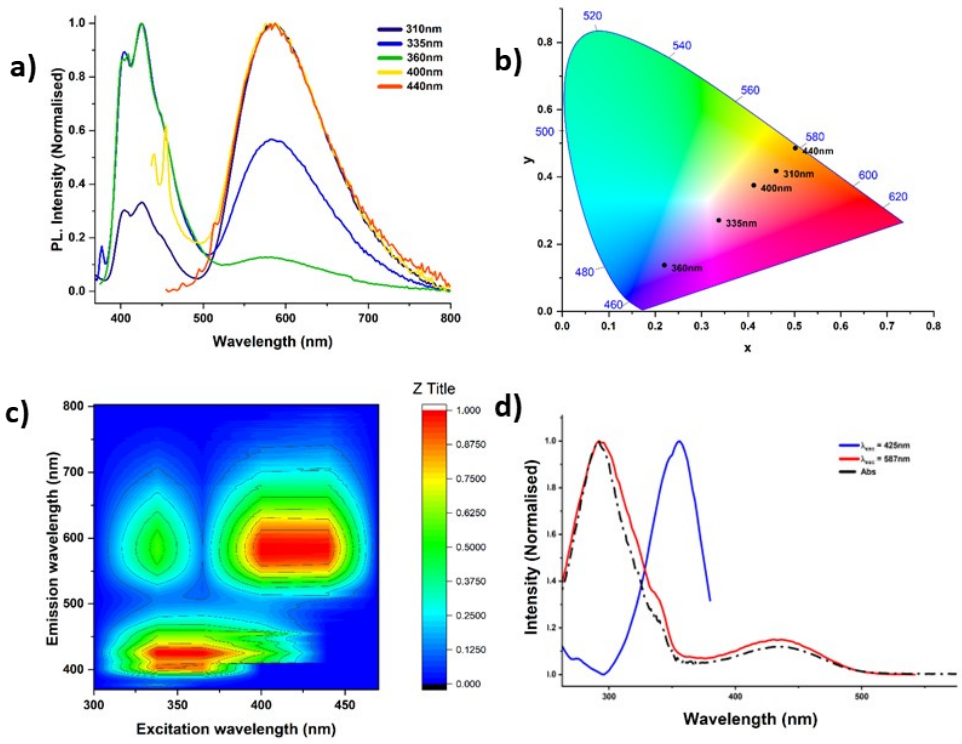

Figure S12. a) Excitation wavelength-dependent emission spectra of compound **1** in CH_3CN at 298 K (c = 10^{-5} M); **b)** CIE plot of excitation wavelength-dependent emission; **c)** 2D-excitation-emission contour plot; **d)** Comparison of absorption and excitation spectra of emissions at 425 nm, 587 nm.

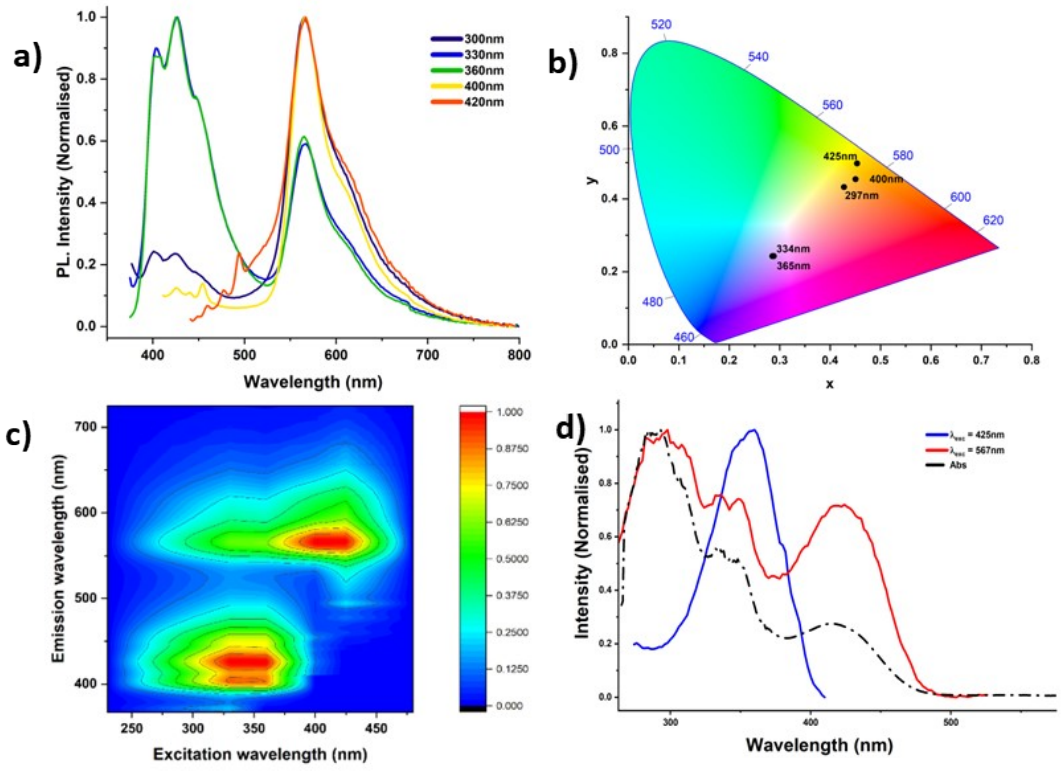

Figure S13. a) Excitation wavelength-dependent emission spectra of compound **2** in CH_3CN at 298 K ($c = 10^{-5}$ M); **b)** CIE plot of excitation wavelength-dependent emission; **c)** 2D-excitation-emission contour plot; **d)** Comparison of absorption and excitation spectra of emissions at 425 nm, 567 nm.

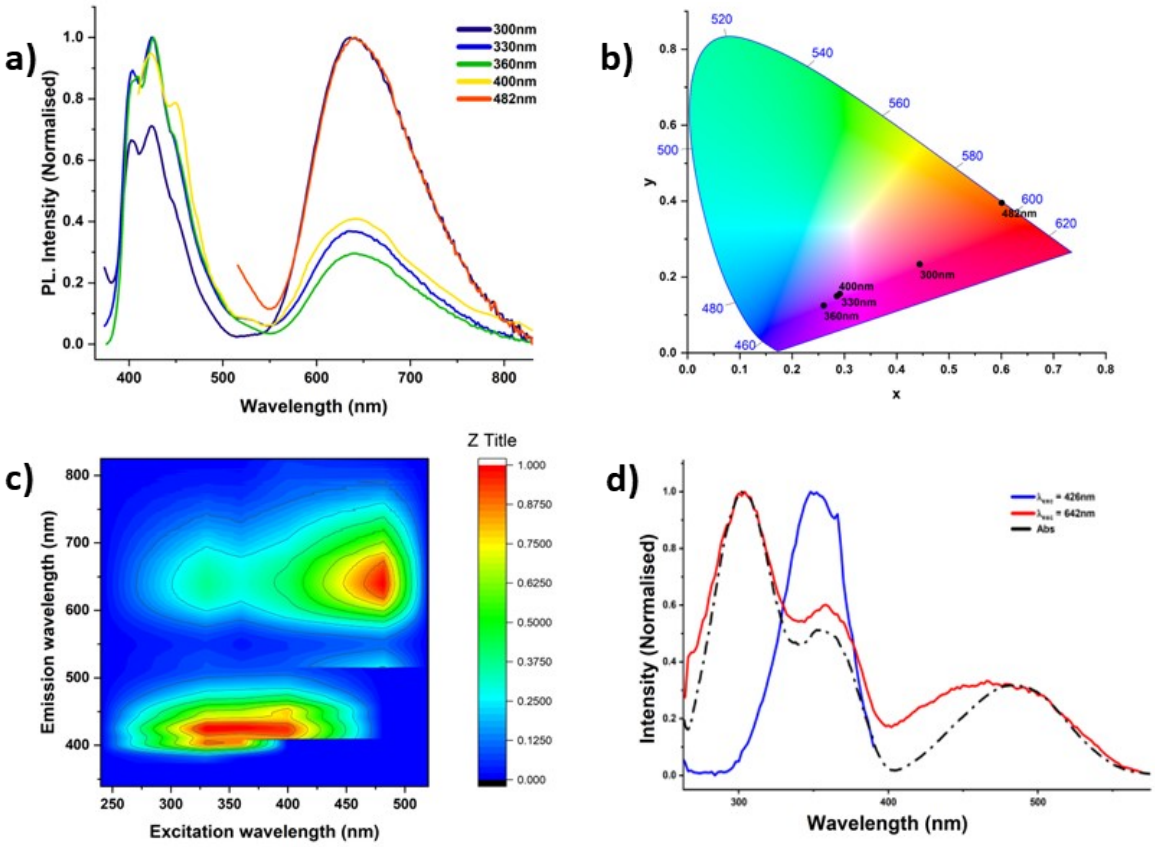

Figure S14. a) Excitation-dependent wavelength emission spectra of compound **3** in CH_3CN at 298 K (c = 10^{-5} M); **b)** CIE plot of excitation wavelength-dependent emission; **c)** 2D-excitation-emission contour plot; **d)** Comparison of absorption and excitation spectra of emissions at 426 nm, 642 nm.

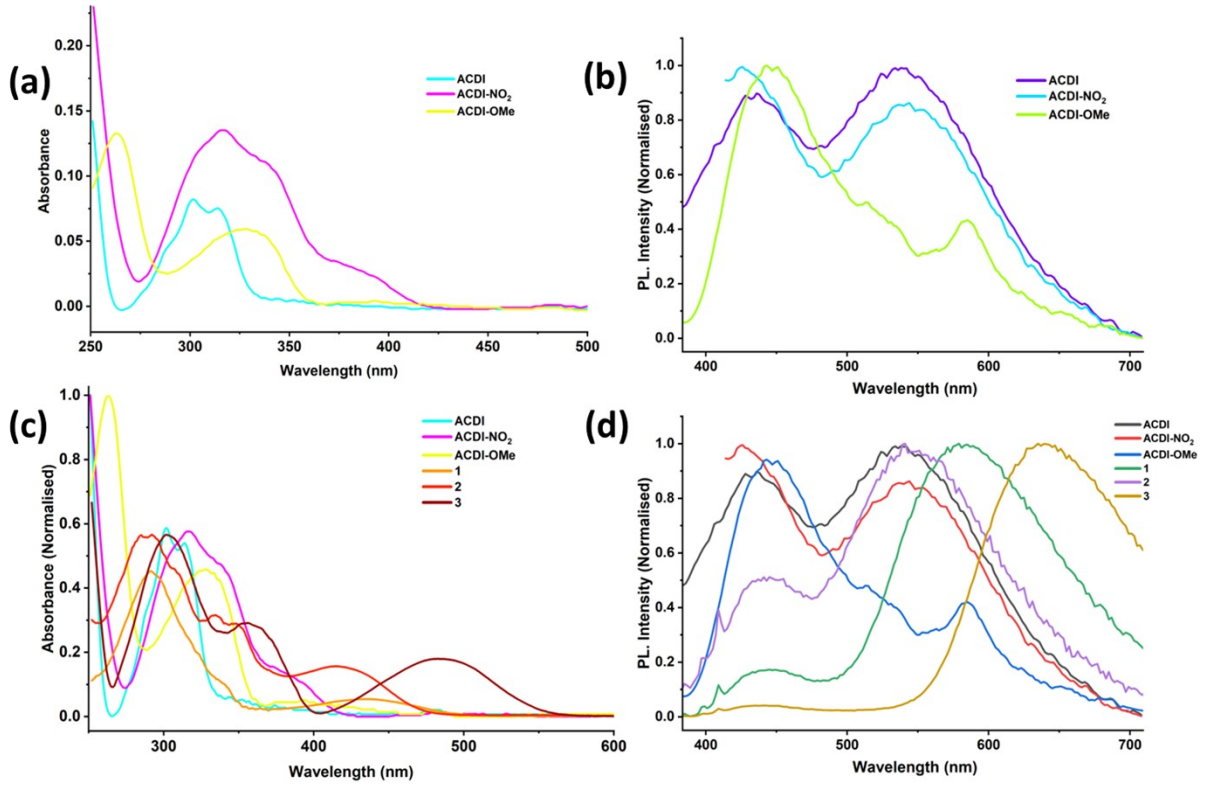

Figure S15. (a) Absorption spectra of precursors in acetonitrile; (b) Normalized emission spectra of precursors ($\lambda_{ex} = \lambda_{max}$) and (c) Normalized absorption spectra of precursors and compounds **1**–**3**; (d) Normalized emission spectra of precursors and compounds **1**–**3** ($c = 10^{-5}$ M), for precursors $\lambda_{ex} = \lambda_{max}$ and for compounds **1**–**3** λ_{ex} = 365 nm. All the measurements were performed in acetonitrile ($c = 10^{-5}$ M) at 298 K.

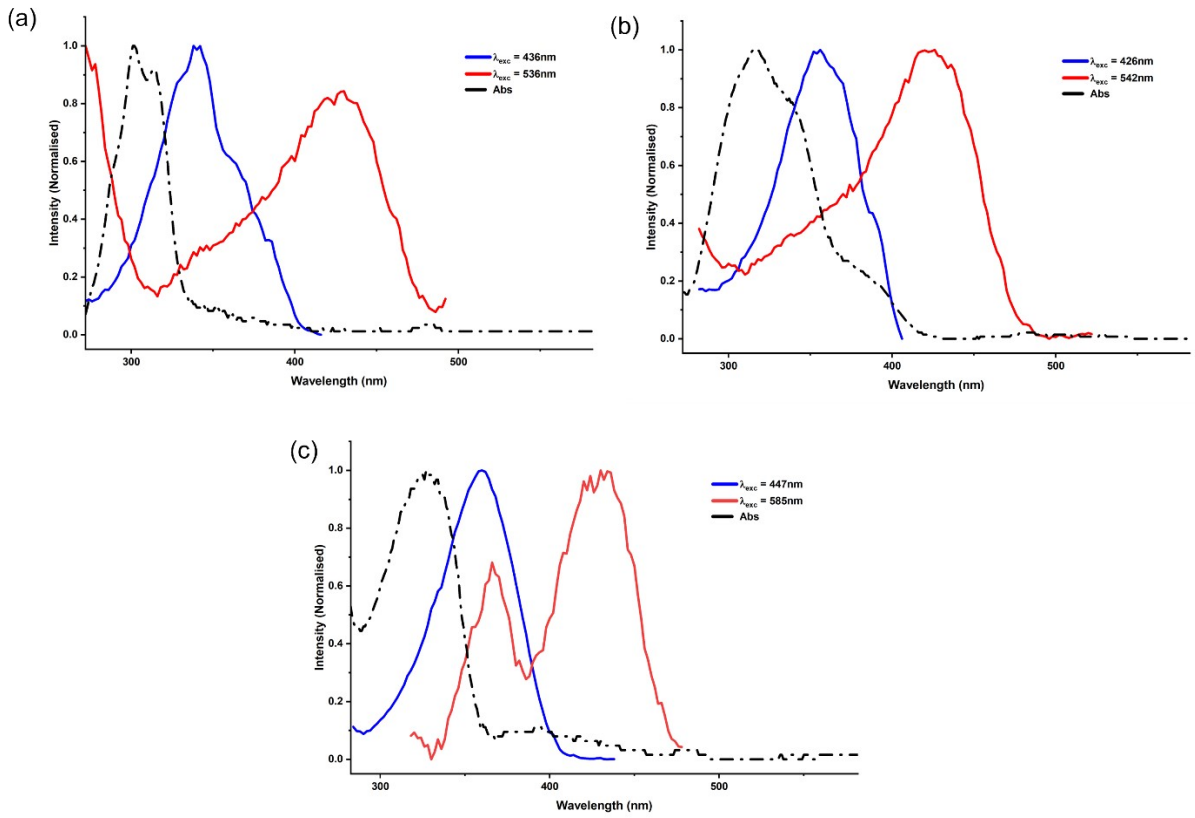

Figure S16. Normalized absorption and excitation spectra of precursors (a) **ACDI**; (b) **ACDI-NO_2** and (c) **ACDI-OMe** in CH_3CN (c =10^{-5} M) at 298 K.

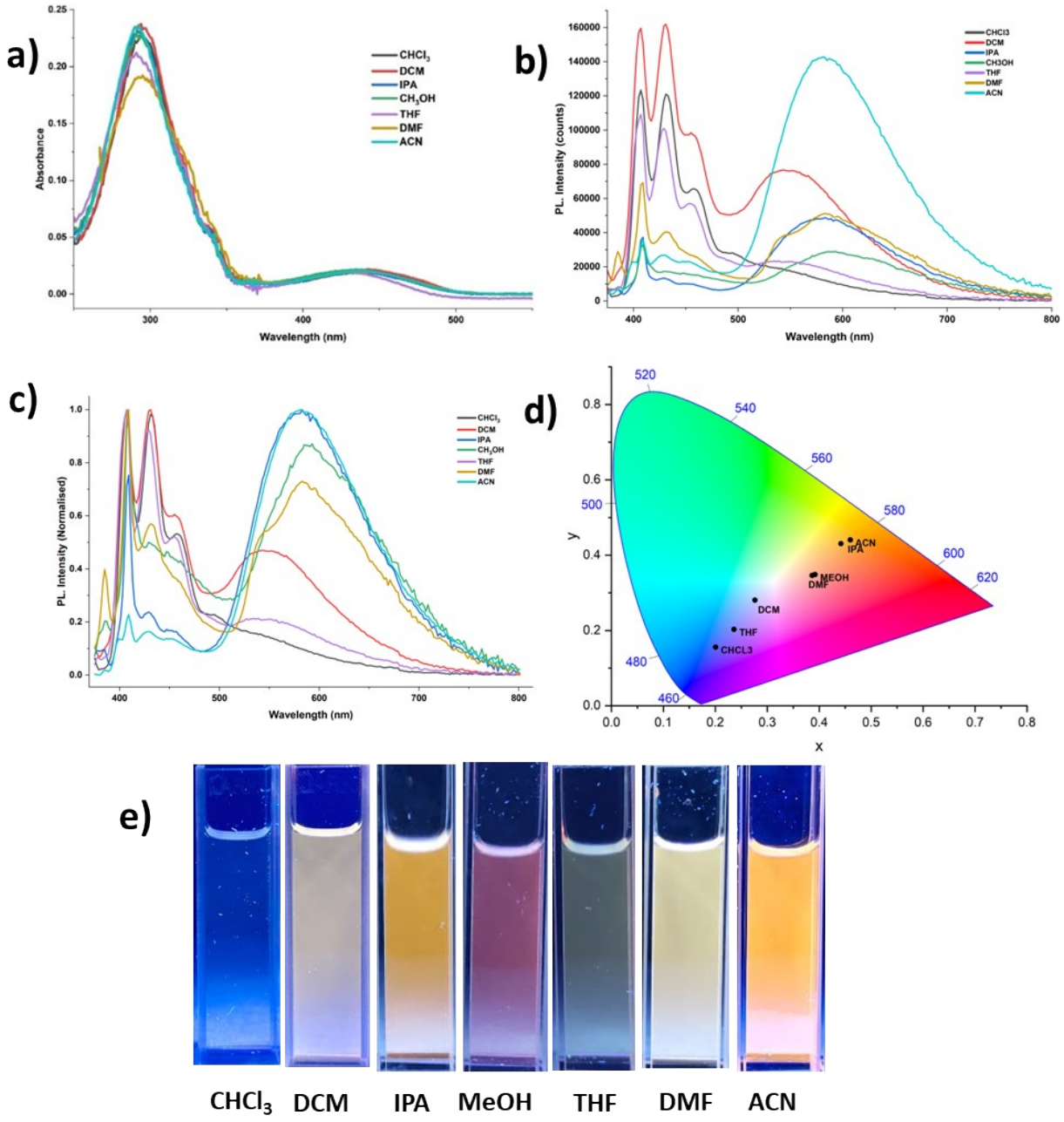

Figure S17. **a)** Absorption spectra of compound **1** (298 K) in different solvents (c = 10^{-5} M); **b)** Emission spectra in different solvents (λ_{ex} = 365 nm); **c)** Normalized emission spectra; **d)** CIE plot; and **e)** Photographs of these solutions taken under 365 nm.

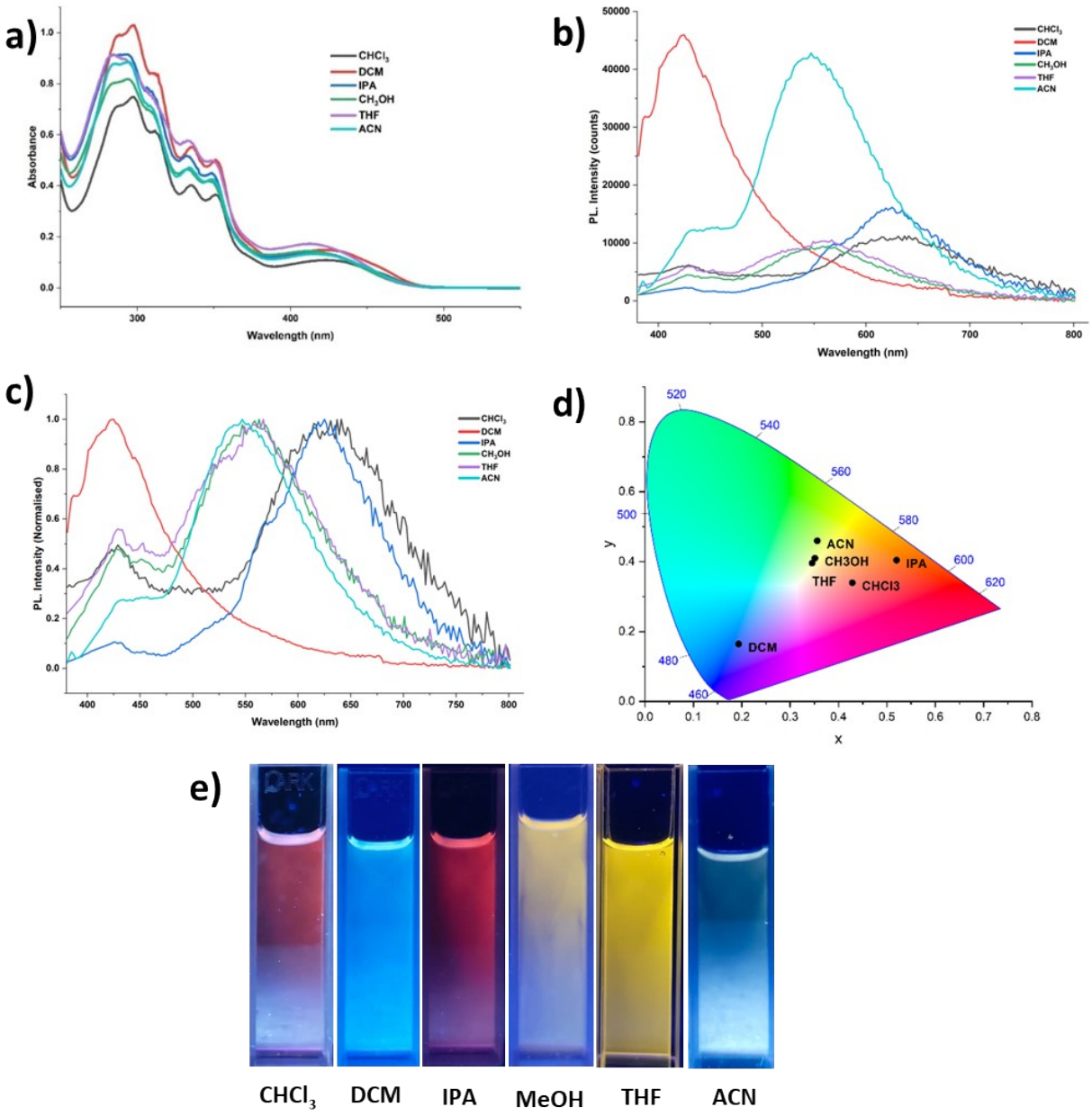

Figure S18. a) Absorption spectra of compound **2** (298 K) in different solvents (c = 10^{-5} M); b) Emission spectra in different solvents (λ_{ex} = 365 nm); c) Normalized emission spectra; d) CIE plot; and e) Photographs of these solutions taken under 365 nm.

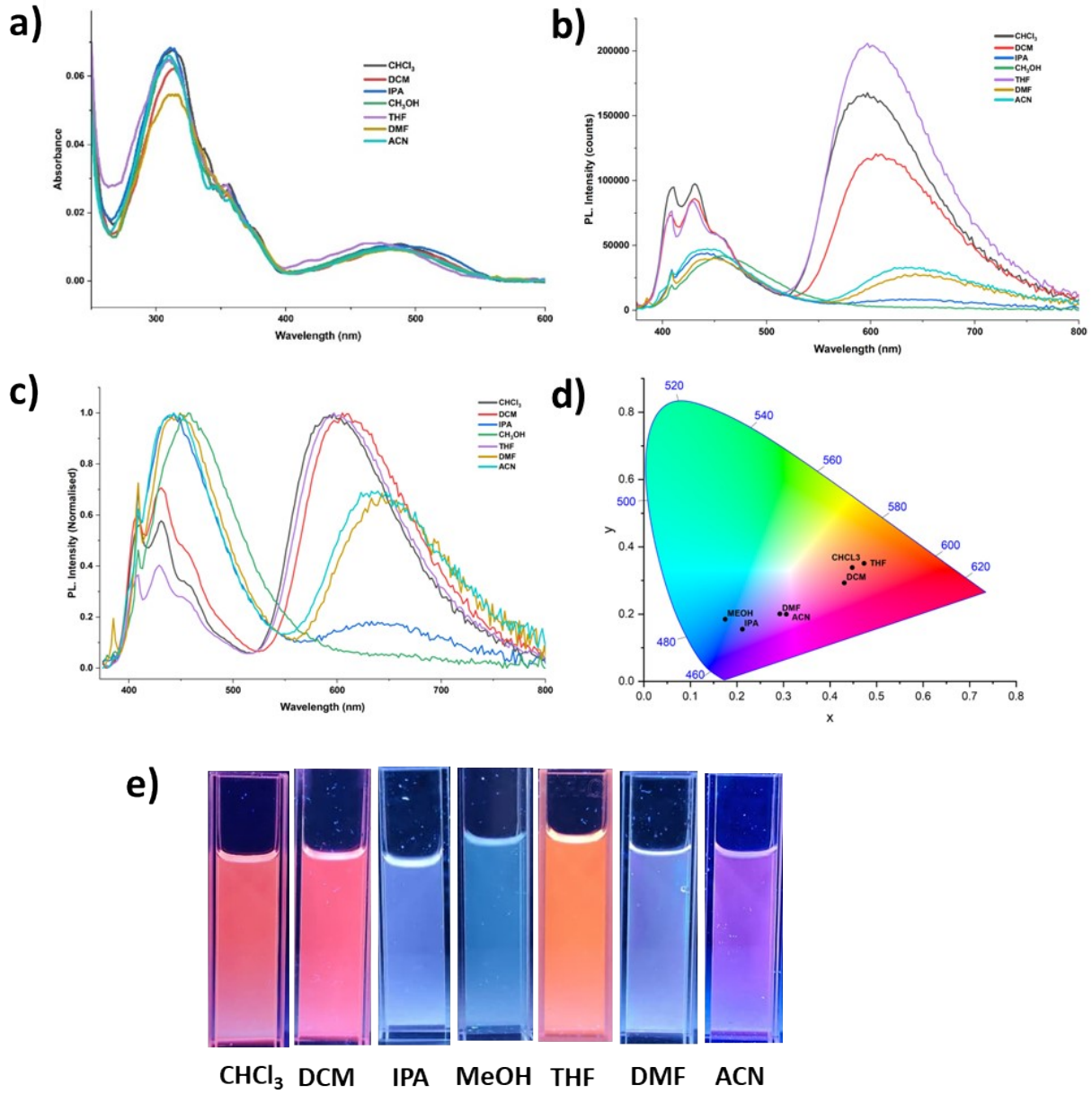

Figure S19. a) Absorption spectra of compound **3** (298 K) in different solvents (c =5 × 10^{-6} M); b) Emission spectra in different solvents (λ_{ex} = 365 nm); c) Normalized emission spectra; d) CIE plot; e) Photographs of these solutions taken under 365 nm.

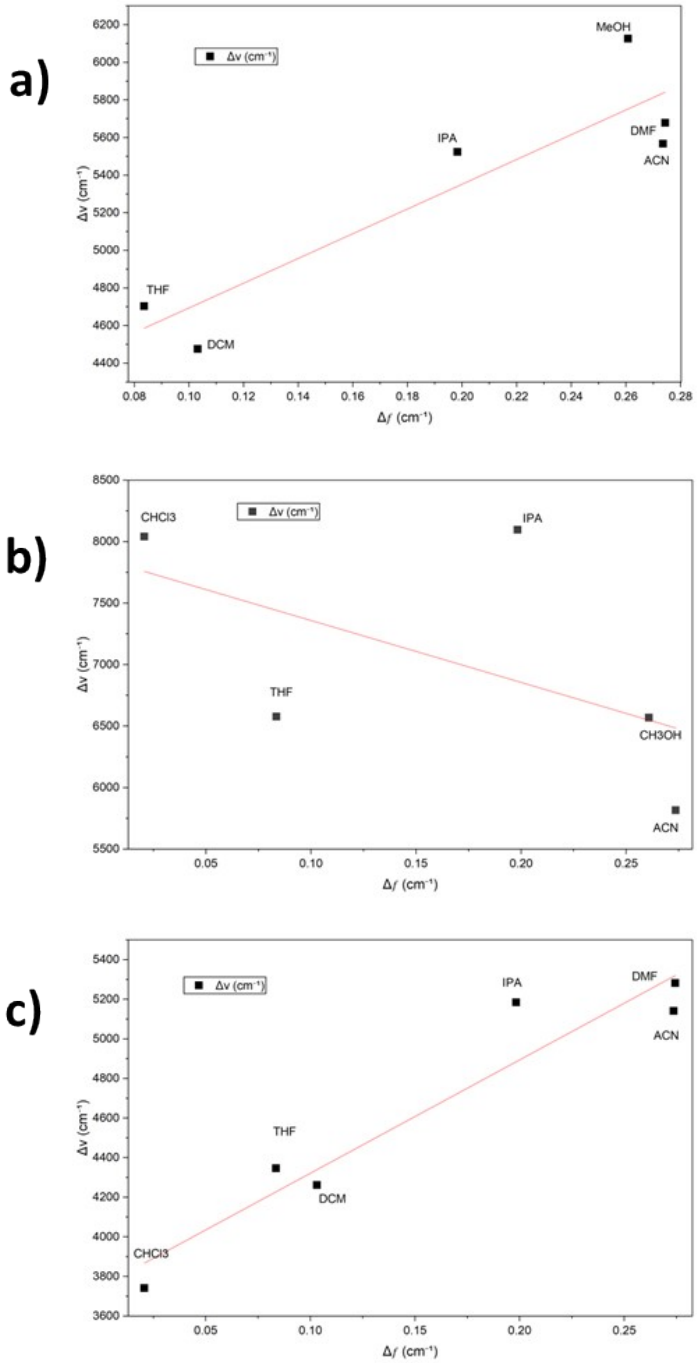

Figure S20. Lippert-Mataga plot of compounds **a) 1**, **b) 2** and **c) 3**.

Table S1. Absorbance and emission maxima, and Stokes' shift data for compounds **1-3**, where absorbance maxima are represented as λ_{abs} in wavelength and νabs in wavenumber, and emission maxima as λ_{em} in wavelength and ν_{em} in wavenumber ($\lambda_{ex} = \lambda_{abs}$).

Compound 1						
Solvent	**λ_{abs} (nm)**	**λ_{em}(nm)**	**$\Delta\lambda$(nm)**	**ν_{abs}(cm^{-1})**	**ν_{em}(cm^{-1})**	**$\Delta\nu$ (cm^{-1})**
$CHCl_3$	443	-	-	22573	-	-
DCM	442	543	101	22624	18146	4470
IPA	441	583	142	22675	17152	5520
CH_3OH	435	593	158	22988	16863	6130
THF	430	539	109	23255	18552	4700
DMF	438	583	145	22831	17152	5680
ACN	439	581	142	22779	17211	5570

Compound 2						
Solvent	**λ_{abs} (nm)**	**λ_{em}(nm)**	**$\Delta\lambda$(nm)**	**ν_{abs}(cm^{-1})**	**ν_{em}(cm^{-1})**	**$\Delta\nu$ (cm^{-1})**
$CHCl_3$	423	641	218	23640	15600	8040
DCM	423	-	-	23640	-	-
IPA	415	625	210	24096	16000	8100
CH_3OH	411	563	152	24330	17761	6570
THF	413	567	154	24213	17636	6580
ACN	415	547	132	24096	18281	5810

Compound 3						
Solvent	**λ_{abs} (nm)**	**λ_{em}(nm)**	**$\Delta\lambda$(nm)**	**ν_{abs}(cm^{-1})**	**ν_{em}(cm^{-1})**	**$\Delta\nu$ (cm^{-1})**
$CHCl_3$	488	597	109	20491	16750	3740
DCM	481	605	124	20790	16528	4260
IPA	480	639	159	20833	15649	5180
CH_3OH	480	-	-	20833	-	-
THF	474	597	123	21097	16750	4350
DMF	480	643	168	20833	15552	5280
ACN	481	639	158	20790	15649	5140

Fluorescence Studies in Thin Film

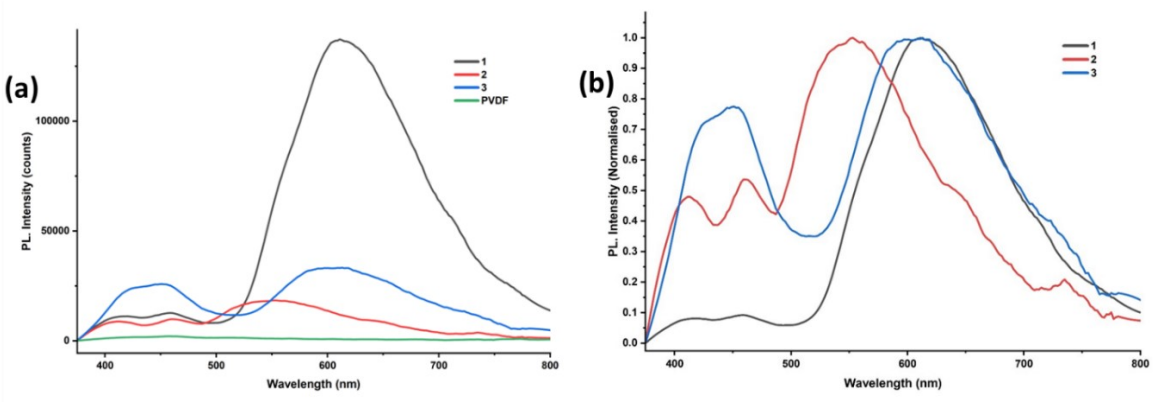

Figure S21. (a) Emission spectra of 5 wt% compounds in polyvinylidene fluoride (PVDF) thin film; (b) its normalized emission spectra, (λ_{ex} = 365 nm).

Solid-state Fluorescence Studies

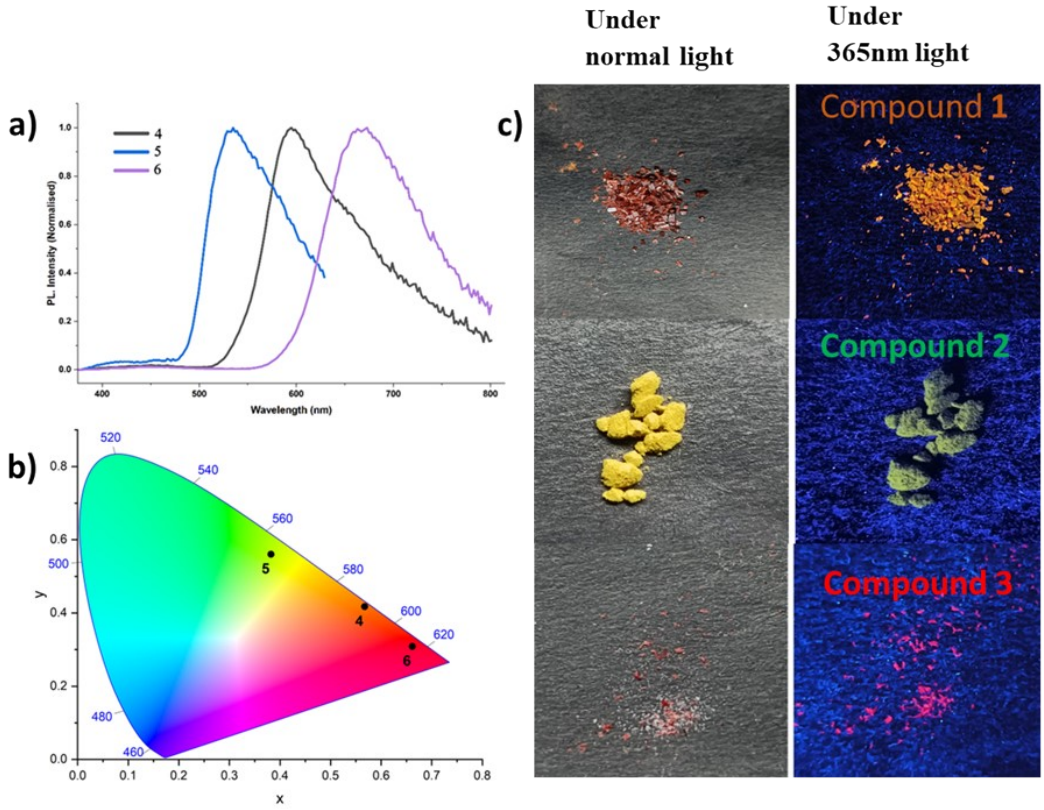

Figure S22. a) Solid-state emission spectra of compounds **1**-**3**; b) its CIE plot; c) Photographs taken under normal light and 365 nm light (λ_{ex} = 365 nm). Although single emission band was

observed for all the compounds (λex = 365 nm) in their solid-state dual emissions were observed in thin film (Figure S21 and S22). In solid-state, strong intermolecular interactions facilitate rapid internal conversion from higher excited state, resulting emission from S_1 state following Kasha's rule. In thin films, fluorophores are away from one another resulting in weak/no intermolecular interaction and thus, emission from higher excited state if feasible.

6. Lifetime measurements

Table S2. Lifetime data of compounds. The short wavelength emission peak was fitted with biexponential decay function, which is due to the presence of two emission bands, one from S_3 and the other from S_1. However, the second emission band was fitted with single exponential decay function as it corresponds to single emission band. For short wavelength emission 380 nm laser pulse (10 ps) was used while for longer wavelength emission 480 nm laser pulse (ns) was employed.

Compounds	Lifetime (short wavelength)		Lifetime (longer wavelength)
	τ_1 (ns)	τ_2 (ns)	τ_1 (ns)
1	1.61 ± 0.01 (84%)	7.68 ± 2.32 (16%)	5.37 ± 0.10 (100%)
2	1.27 ± 0.23 (83%)	4.04 ± 2.17 (17%)	1.67 ± 0.04 (100%)
3	1.57 ± 0.03 (86%)	8.49 ± 0.7 (14%)	1.41 ± 0.12 (100%)

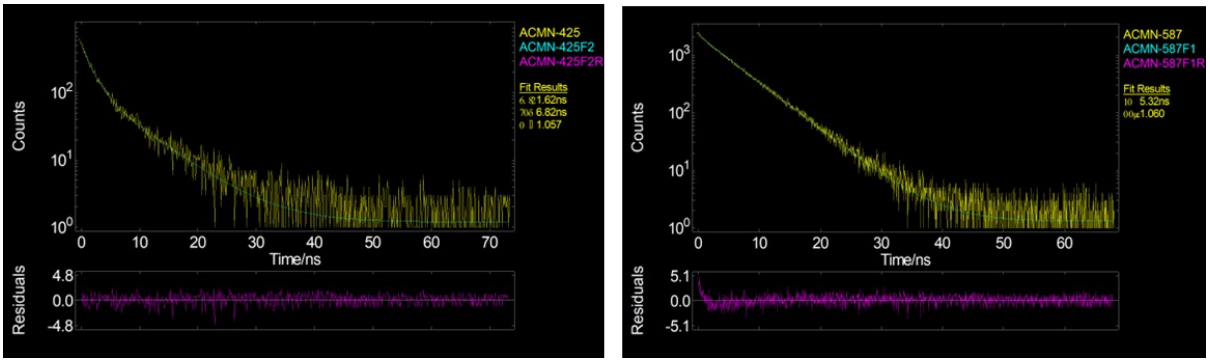

Figure S23. Lifetime plot of compound **1** (298 K) in CH_3CN ($c = 10^{-5}$ M).

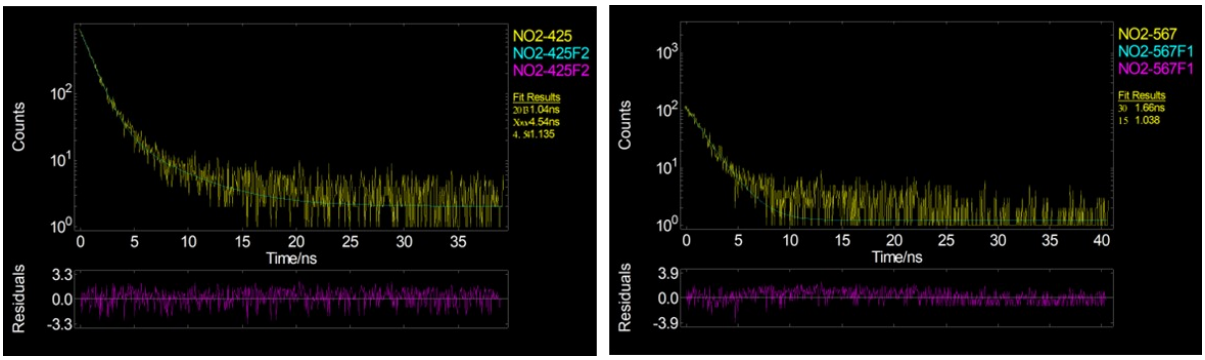

Figure S24. Lifetime plot of compound **2** (298 K) in CH_3CN ($c = 10^{-5}$ M).

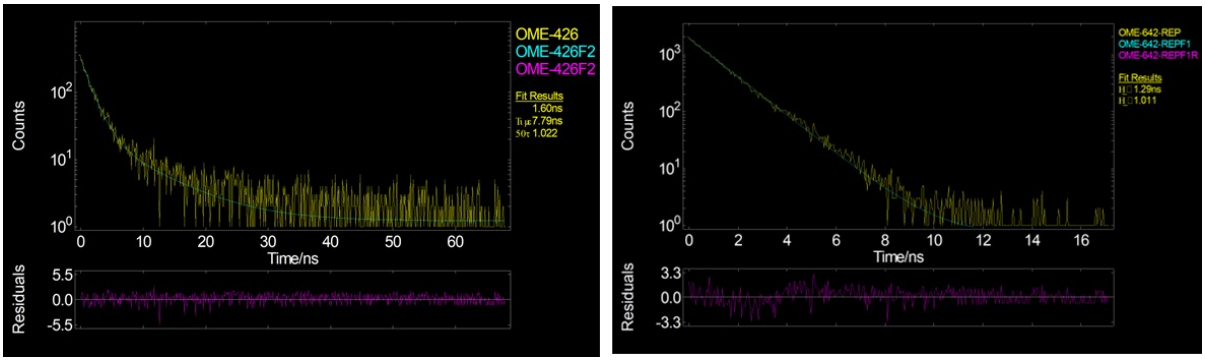

Figure S25. Lifetime plot of compound **3** (298 K) in CH_3CN ($c = 10^{-5}$ M).

7. Quantum yield Measurements:

The quantum yields were determined relative to the reference compounds Rhodamine B and 9,10-diphenyl anthracene. Based on the following equation, the quantum yields were calculated, where subscripts ST and X denote 'standard' and 'test', respectively, Φ denotes the fluorescence quantum yield, Grad denotes the gradient derived from the plot of integrated fluorescence intensity versus absorbance, and η denotes the refractive index of the solvents. 1.361 and 1.344 were used as the refractive indices of ethanol and acetonitrile.

$$\Phi_X = \Phi_{ST} \times \left[\frac{Grad_X}{Grad_{ST}}\right] \times \left[\frac{\eta^2_X}{\eta^2_{ST}}\right]$$

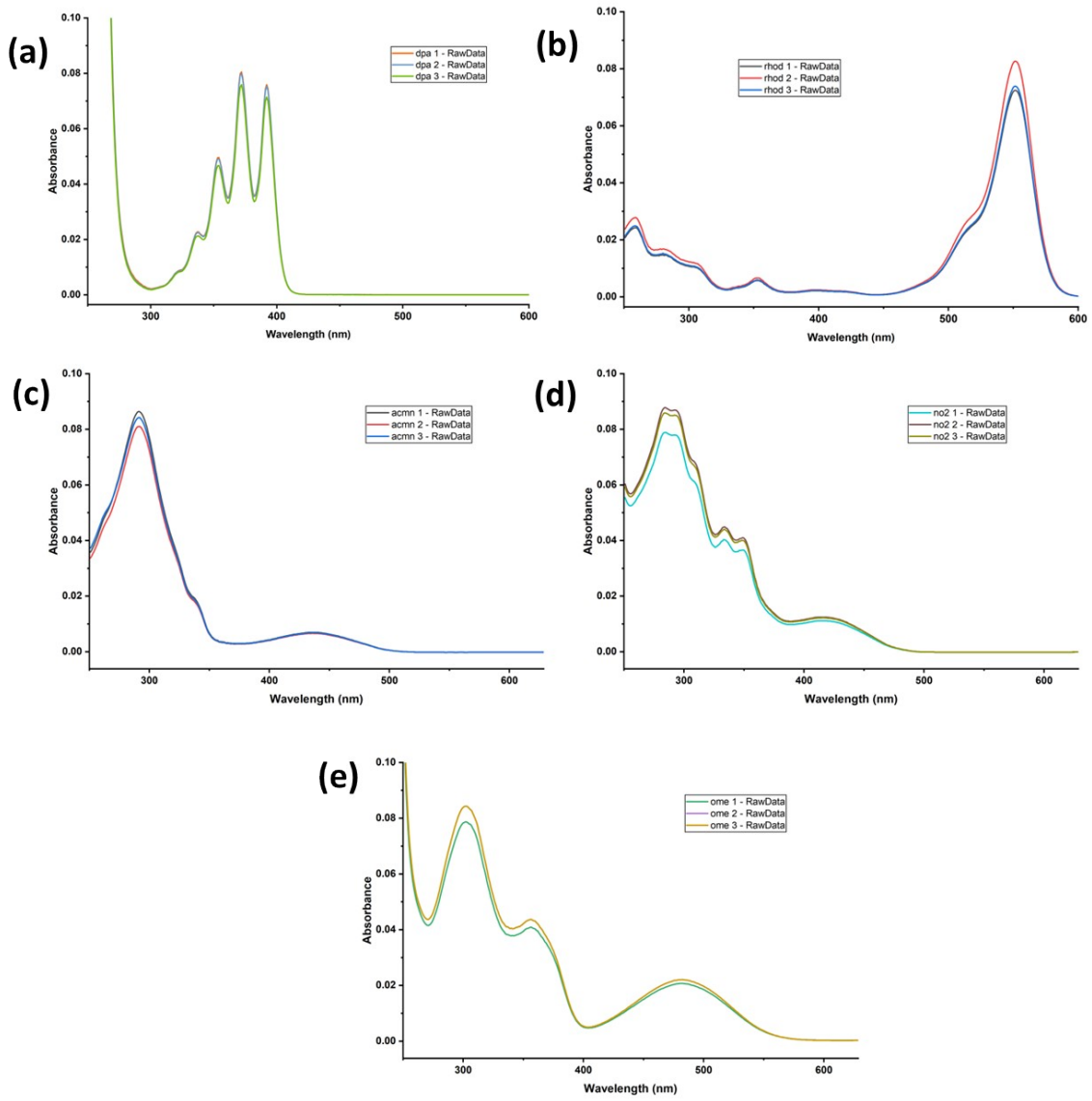

Figure S26. UV-Vis spectra of (a) DPA in ethanol; (b) Rhodamine-B in ethanol; (c) compound **1** in CH_3CN; (d) compound **2** in CH_3CN and (e) compound **3** in CH_3CN.

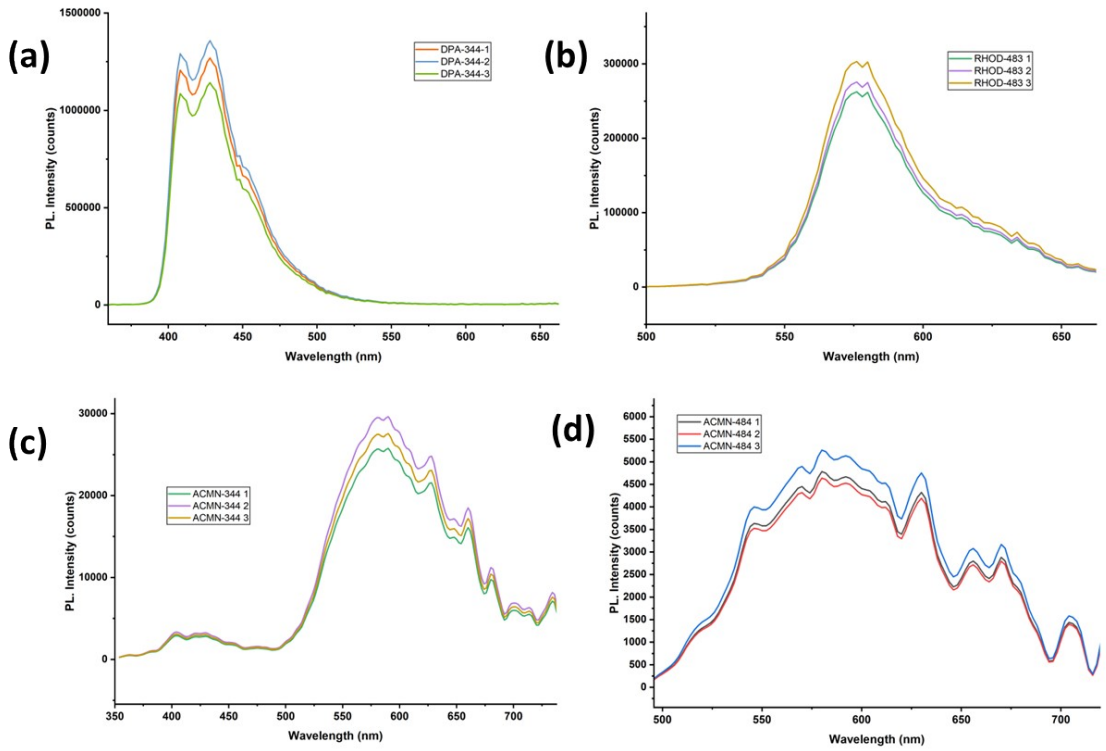

Figure S27. PL spectra of (a) DPA excitation at 344 nm in ethanol; (b) Rhodamine-B excitation at 483 nm in ethanol; (c) compound **1** excitation at 344 nm in CH_3CN; (d) compound **1** excitation at 484 nm in CH_3CN.

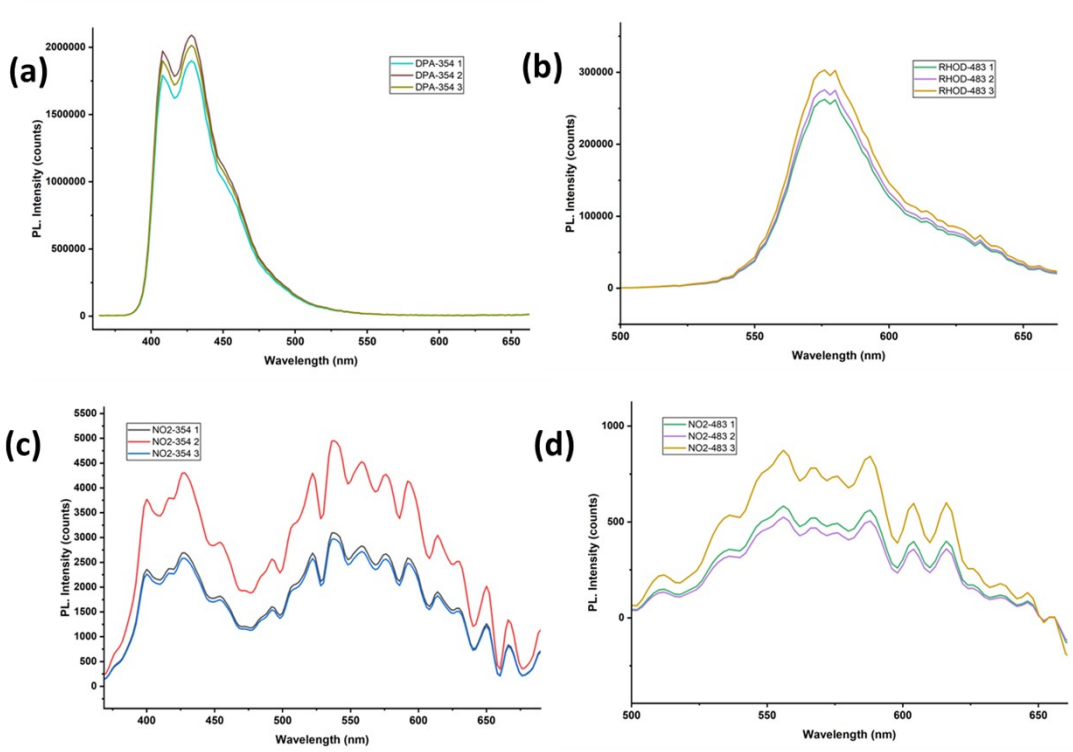

Figure S28. PL spectra of (a) DPA excitation at 354 nm in Ethanol; (b) Rhodamine-B excitation at 483 nm in Ethanol; (c) compound **2** excitation at 354 nm in CH_3CN; (d) compound 5 excitation at 483 nm in CH_3CN.

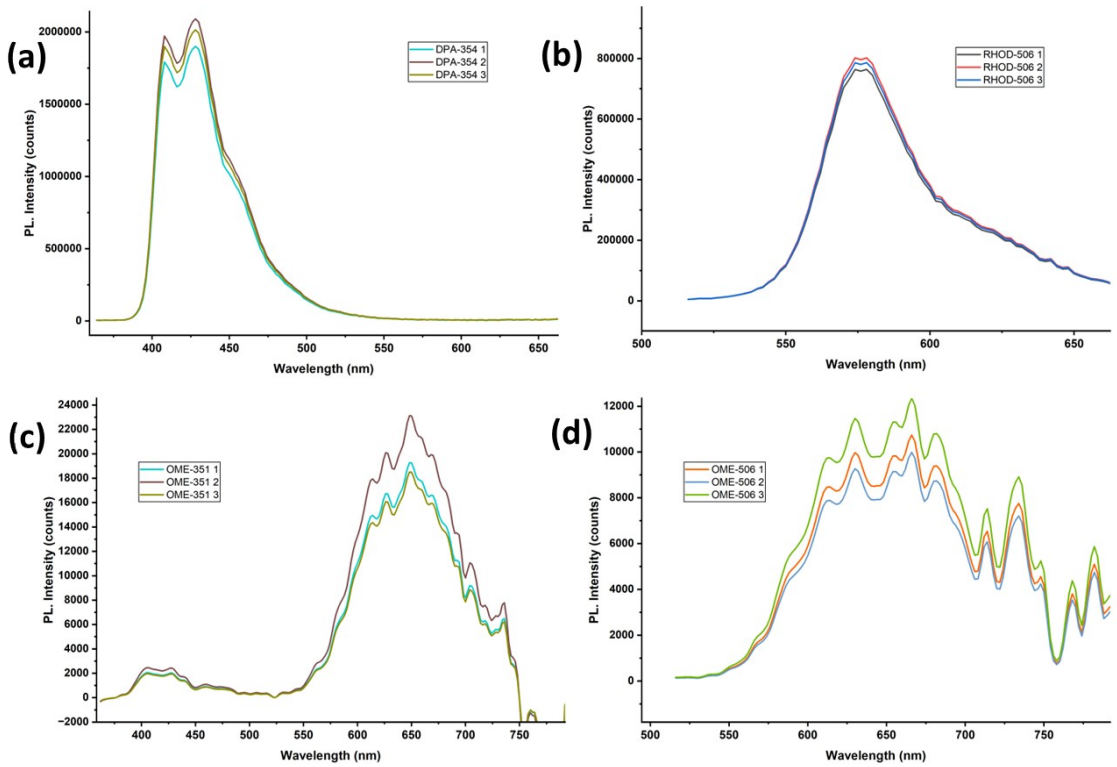

Figure S29. PL spectra of (a) DPA excitation at 354 nm in Ethanol; (b) Rhodamine-B excitation at 506 nm in Ethanol; (c) compound **3** excitation at 351 nm in CH_3CN; (d) compound **3** excitation at 506 nm in CH_3CN.

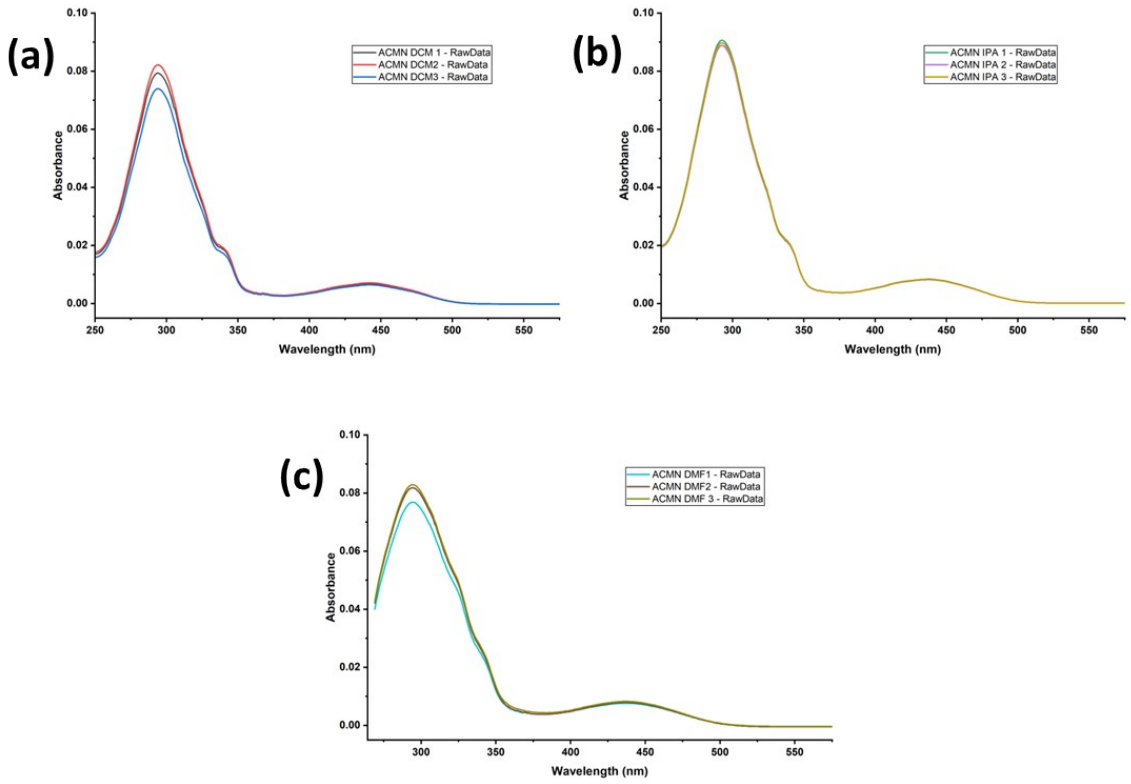

Figure S30. UV-Vis spectra of (a) compound **1** in DCM; (b) IPA and (c) DMF

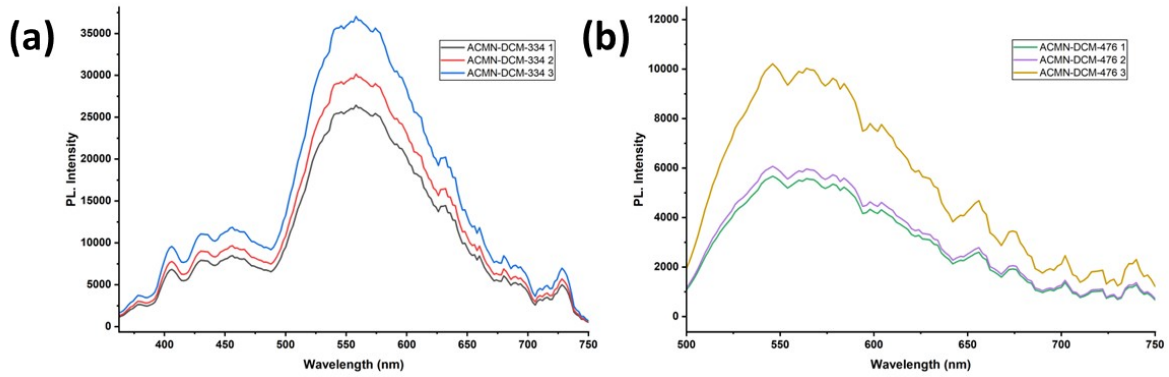

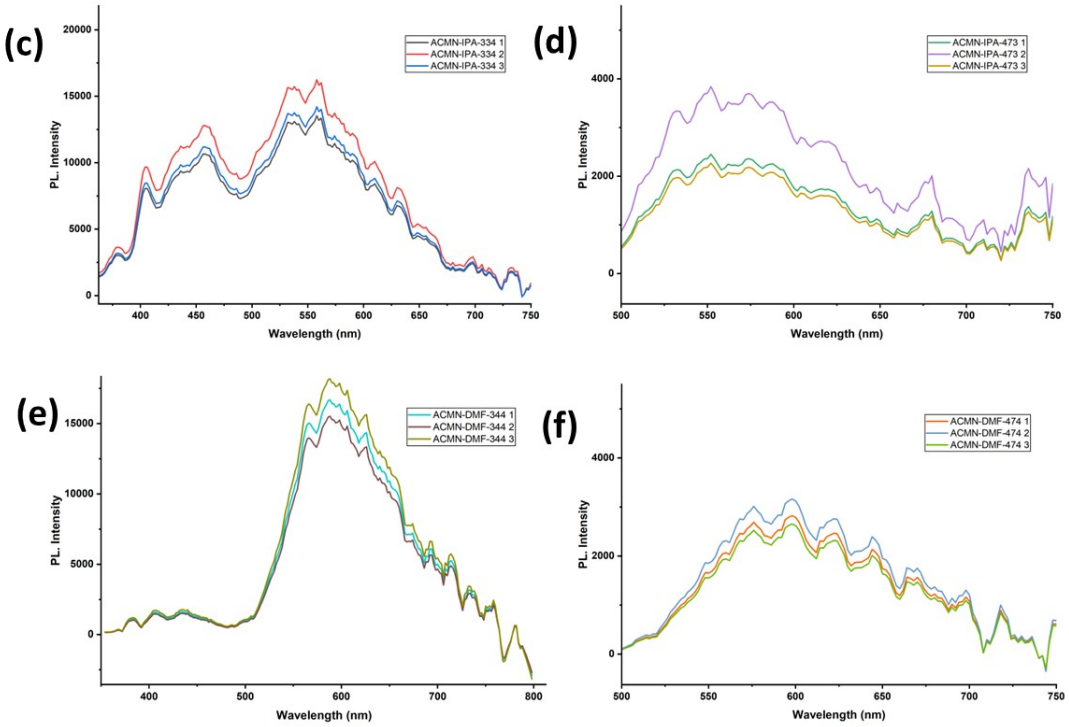

Figure S31. PL spectra of compound **1** (a) excitation at 334 nm in DCM; (b) excitation at 476 nm in DCM; (c) excitation at 334 nm in IPA; (d) excitation at 473 nm in IPA; (e) excitation at 344 nm in DMF; (f) excitation at 474 nm in DMF.

Table S3. Summary of Quantum yield of compound **1**.

Quantum yield of compound **1**	
ACN	7.45 ± 0.21, 5.56 ± 0.31
DCM	4.27 ± 0.11, 2.35 ± 0.17
IPA	3.63 ± 0.25, 0.90 ± 0.07
DMF	3.57 ± 0.31, 1.84 ± 0.22

Table S4. Summary of photophysical studies of precursors and compounds **1-3** in CH_3CN.

Compounds	Solution				Solid
	λ_{abs} (nm)	λ_{em} (nm)	τ_{FL} (ns)	Φ_{FL}	λ_{em} (nm)
ACDI	301	436,538	-	-	-
ACDI-NO_2	317	426,544	-	-	-
ACDI-OMe	263, 327	443,585	-	-	-
1	290, 410, 435	425,587	1.61 ± 0.01, 5.37 ± 0.10	7.45 ± 0.21, 5.56 ± 0.31	595
2	290, 336, 414	425,567	1.27 ± 0.23, 1.67 ± 0.04	2.64 ± 0.39, 1.14 ± 0.29	535
3	303, 455, 482	426,642	1.57 ± 0.03, 1.41 ± 0.12	5.15 ± 0.19, 2.84 ± 0.30	673

8. Crystallographic Information

Single crystals suitable for diffraction were obtained by the slow evaporation of acetonitrile from their solutions. Data were collected on a Bruker D8 Quest diffractometer with Mo Kα (λ = 0.71073) radiation. Data reduction was performed using the Bruker AXS SAINT and SADABS programs. The structures were solved by direct methods using SHELXT 2018. Mercury software was utilized for molecular representations in the diagrams. The CIF file is submitted to CCDC and can be obtained through https://summary.ccdc.cam.ac.uk/structure-summary-form.

Table S5. Single crystal data of compound **1**.

Identification code	**1**
Molecular formula	$C_{15}H_6N_2O$
Formula weight	230.05 g/mol
Temperature/K	273K
Crystal system	triclinic
Space group	P -1
a/Å	10.1201 (5)
b/Å	16.0962 (7)
c/Å	20.8415 (10)
α/°	89.550 (2)
β/°	82.058 (2)
γ/°	79.000 (1)
Volume/Å^3	3300.0 (3)
Z	2
ρ_{calc} g/cm^3	1.394
μ/mm^{-1}	0.091
F (000)	1420.0
Crystal size/mm^3	0.22 × 0.18 × 0.13
Radiation	Mo Kα (λ = 0.71073)
2Θ range for data collection/°	3.948 to 54.308
Index ranges	-12 ≤ h ≤ 12, -20 ≤ k ≤ 20, -26 ≤ l ≤ 26

Reflections collected	98561
Independent reflections	14582 [R_{int} = 0.0524, R_{sigma} = 0.0350]
Data/restraints/parameters	14582/0/973
Goodness-of-fit on F^2	1.368
Final R indexes [I>=2σ (I)]	R_1 = 0.0681, wR_2 = 0.1961
Final R indexes [all data]	R_1 = 0.0962, wR_2 = 0.2067
Largest diff. peak/hole / e Å^{-3}	0.33/-0.47

Table S6. Single crystal data of compound **3**.

Identification code	**3**
Molecular formula	$C_{16}H_8N_2O_2$
Formula weight	260.24 g/mol
Temperature/K	303K
Crystal system	monoclinic
Space group	$P2_1/c$
a/Å	6.994 (3)
b/Å	16.658 (6)
c/Å	20.028 (8)
α/°	90
β/°	95.265 (15)
γ/°	90

Volume/Å^3	2323.5
Z	4
ρ_{calc} g/cm^3	1.488
μ/mm^{-1}	0.101
F (000)	1072
Crystal size/mm^3	0.195 × 0.158 × 0.015
Radiation	Mo Kα (λ = 0.71073)
2Θ range for data collection/°	4.048 to 54.204
Index ranges	-8 ≤ h ≤ 8, -20 ≤ k ≤ 21, -25 ≤ l ≤ 25
Reflections collected	45810
Independent reflections	5099 [R_{int} = 0.0923, R_{sigma} = 0.0580]
Data/restraints/parameters	5099/0/363
Goodness-of-fit on F^2	1.057
Final R indexes [I>=2σ (I)]	R_1 = 0.0810, wR_2 = 0.2206
Final R indexes [all data]	R_1 = 0.1049, wR_2 = 0.2470
Largest diff. peak/hole / e Å^{-3}	0.65/-0.37

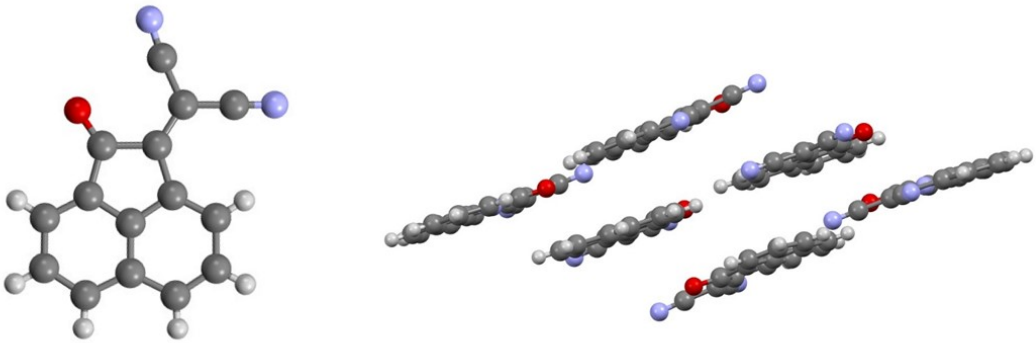

Figure S32. Single crystal structure and packing of compound **1**.

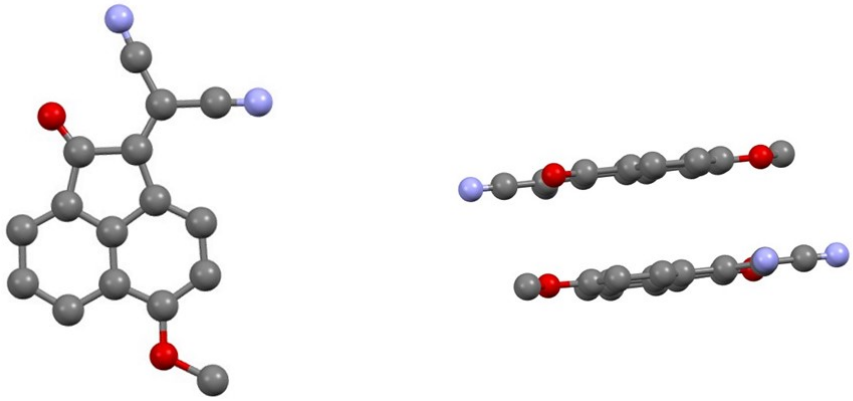

Figure S33. Single crystal structure and packing of compound **3**.

9. DFT Calculation

All theoretical calculations were performed using the Gaussian 16, Revision A.03. Geometries were optimized in acetonitrile with the PCM solvation model by PBE1PBE 6-311+g(d,p). Vibrational frequencies were calculated at the same level as the optimized structure. Density functional theory (DFT) and time-dependent DFT (TDDFT) calculations were performed using the PBE functional and 6-311+g(d,p) basis set. The comparison table of experimental and calculated data, ground and excited states optimized structures are given below.

Table S7. Comparison of photophysical properties between experimental and calculated data.

Compounds	Absorbance		Emission	
	λ_{max}(nm) Experimental	λ_{max}(nm) Theoretical	λ_{max}(nm) experimental	λ_{max}(nm) Theoretical
1	290, 337, 435	314, 333, 486	425, 587	468, 610
2	290, 336, 414	323, 358, 470	425, 567	444, 578
3	303, 355, 482	321, 366, 531	426, 642	445, 665

9.1 Compound **1** Gaussian optimization

Ground state optimization

opt freq=noraman PBE1PBE/6-311+g(d,p) scrf=(solvent=acetonitrile,pcm) geom=connectivity scf=(tight,maxcycle=1000)

Cartesian coordinates of the structures

C	-1.05495300	-0.11505300	-0.00004600
C	-0.45107100	-1.52543300	-0.00006000
O	-1.09039300	-2.54893200	-0.00011700
C	1.23998400	0.05225100	0.00006600
C	2.52550300	0.61011200	0.00013500
C	0.04753700	0.82368400	0.00003800
C	0.15284200	2.20068300	0.00008200
H	-0.71872500	2.84357100	0.00006500
C	2.59594600	2.02487400	0.00017900
C	1.44001000	2.78069400	0.00015300

H	1.51769100	3.86222700	0.00018700
H	3.56382000	2.51580600	0.00023200
C	1.00833900	-1.33299100	0.00001200
C	3.60499400	-0.30776300	0.00015000
C	2.06788500	-2.20901000	0.00002700
H	1.91486700	-3.28268400	-0.00001400
C	3.37345500	-1.67016800	0.00009800
H	4.21942000	-2.34854300	0.00011100
H	4.62384900	0.06632400	0.00020300
C	-2.39651500	0.09929200	-0.00010800
C	-2.94674800	1.41257400	-0.00008500
C	-3.36673700	-0.94721800	-0.00020500
N	-4.23406500	-1.70938700	-0.00028800
N	-3.40030800	2.47447100	-0.00006400

S_1 excited state optimization

opt=calcfc freq=noraman td=(nstates=10,root=1,read) PBE1PBE /6-311+g(d,p) scrf=(solvent=acetonitrile,pcm) pbe1pbe scf=(tight,maxcycle=1000)

Cartesian coordinates of the structures

C	-1.05215900	-0.18672100	-0.00005900
C	-0.47068800	-1.51671500	-0.00007800
O	-1.03760500	-2.60597100	-0.00013800
C	1.25805900	0.05957100	0.00006000
C	2.53364700	0.63073500	0.00013700
C	0.04558500	0.78459500	0.00002000

C	0.13924600	2.18370900	0.00005900
H	-0.74114100	2.81361400	0.00003000
C	2.59815000	2.03655400	0.00017900
C	1.40527200	2.77582900	0.00013900
H	1.46852300	3.85819300	0.00017200
H	3.55454300	2.54775700	0.00023800
C	1.02070400	-1.31203500	0.00000200
C	3.61898600	-0.27429600	0.00016300
C	2.10448000	-2.19776600	0.00003000
H	1.95123400	-3.27101400	-0.00001000
C	3.39007000	-1.66071700	0.00010900
H	4.24436200	-2.32741100	0.00012900
H	4.63719300	0.10003000	0.00022500
C	-2.42643300	0.09231900	-0.00010300
C	-2.93558800	1.40620800	-0.00004900
C	-3.41895600	-0.91460200	-0.00020700
N	-4.29863100	-1.67103500	-0.00029400
N	-3.36938900	2.48340500	-0.00000500

S_3 excited state optimization

opt=calcfc freq=noraman td=(nstates=20,root=3,read) PBE1PBE /6-311+g(d,p) scrf=(solvent=acetonitrile,pcm) scf=(tight,maxcycle=1000)

Cartesian coordinates of the structures

C	-1.05215900	-0.18672100	-0.00005900
C	-0.47068800	-1.51671500	-0.00007800

O	-1.03760500	-2.60597100	-0.00013800
C	1.25805900	0.05957100	0.00006000
C	2.53364700	0.63073500	0.00013700
C	0.04558500	0.78459500	0.00002000
C	0.13924600	2.18370900	0.00005900
H	-0.74114100	2.81361400	0.00003000
C	2.59815000	2.03655400	0.00017900
C	1.40527200	2.77582900	0.00013900
H	1.46852300	3.85819300	0.00017200
H	3.55454300	2.54775700	0.00023800
C	1.02070400	-1.31203500	0.00000200
C	3.61898600	-0.27429600	0.00016300
C	2.10448000	-2.19776600	0.00003000
H	1.95123400	-3.27101400	-0.00001000
C	3.39007000	-1.66071700	0.00010900
H	4.24436200	-2.32741100	0.00012900
H	4.63719300	0.10003000	0.00022500
C	-2.42643300	0.09231900	-0.00010300
C	-2.93558800	1.40620800	-0.00004900
C	-3.41895600	-0.91460200	-0.00020700
N	-4.29863100	-1.67103500	-0.00029400
N	-3.36938900	2.48340500	-0.00000500

Table S8. Calculated absorption represented as ΔE in eV, oscillation strengths (f), orbital composition and transition dipole moments (μ) and dipole square (μ2) of low-lying states of compound **1** (H_0, H_1, H_2, H_3, H_4 represent HOMO, HOMO-1 HOMO-2, HOMO-3 and HOMO-4 orbitals, respectively. L_0, and L_1 correspond to LUMO, and LUMO-1 respectively. Calculations were performed in acetonitrile using PBE functional and 6-311+g(d,p) basis set.

Excited state	**Δ*E*(eV)**	***f***	**composition**	**μ (X, Y, Z)**	**μ^2**
S_1	2.5463	0.0982	H_0-L_0	(1.2384, 0.2002, 0.0001)	1.5737
S_2	3.0244	0.0000	H_3-L_0 H_3-L_1	(0.0000, 0.0000, -0.0082)	0.0001
S_3	3.3550	0.0281	H_1-L_0	(0.5723, -0.1191, 0.0000)	0.3418
S_4	3.7141	0.2996	H_2-L_1	(-1.7424, -0.5064, -0.0001)	3.2924
S_5	3.9364	0.8661	H_4-L_0	(-2.9929, -0.1527, -0.0001)	8.9805
S_6	4.2517	0.1278	H_2-L_1	(-0.2664, 1.0750, 0.0000)	1.2267

Table S9. Calculated fluorescence represented as ΔE in eV, oscillation strengths (*f*), orbital composition and transition dipole moments (μ) and dipole square (μ^2) of low-lying states of **compound 1** (H_0, and H_1 represent HOMO, and HOMO-1 orbitals, respectively. L_0 corresponds to LUMO. Calculations were performed in acetonitrile using PBE functional and 6-311+g(d,p) basis set.

Excited state	**Δ*E*(eV)**	***f***	**composition**	**μ (X, Y, Z)**	**μ^2**
S_1	2.0324	0.0681	H_0-L_0 (99%)	(1.1550, 0.1837, 0.0001)	1.3678
S_3	3.0170	0.0239	H_1-L_0 (99%)	(0.5543, -0.1243, 0.0000)	0.3227

9.2 Compound **2** Gaussian optimization

Ground state optimization

opt freq=noraman PBE1PBE/6-311+g(d,p) geom=connectivity scrf=(pcm,solvent=acetonitrile) scf=(tight,maxcycle=1000)

Cartesian coordinates of the structures

C	-2.97811100	-0.74174100	-0.00000700
C	0.12560700	-1.79508600	-0.00003700
C	-0.43891900	-0.53951900	-0.00003600
C	0.40917800	0.59986500	-0.00001600
C	1.81676200	0.55091200	0.00001200
C	2.34277100	-0.77664500	0.00000900
C	1.52669100	-1.88906600	-0.00001700
H	-0.46356800	-2.70249800	-0.00005000
C	-0.31494500	1.80636000	-0.00002500
H	1.99440500	-2.86487200	-0.00001800
C	1.74531200	2.98769000	0.00004300
C	0.33774600	3.01305700	0.00000700
H	2.28737400	3.92676200	0.00006700
H	-0.20380400	3.95226000	-0.00000100
C	-1.80975800	-0.05565500	-0.00003900
C	-1.74750000	1.46896300	-0.00008400
O	-2.70422600	2.20270800	0.00005800
C	-4.26040200	-0.11243000	-0.00001600
N	-5.34191000	0.29004000	-0.00002400
C	-3.02195300	-2.16597200	0.00003800
N	-3.06819700	-3.31911300	0.00007600

N	3.78640800	-1.03991900	0.00003000
O	4.15911200	-2.19757000	0.00001000
O	4.54310400	-0.08689400	-0.00005400
C	2.47067600	1.81071600	0.00004400
H	3.54864600	1.85665100	0.00007100

S_1 excited state optimization

opt=calcfc freq=noraman td=(nstates=10,root=1,read) PBE1PBE /6-311+g(d,p)scrf=(solvent=acetonitrile,pcm) scf=(tight,maxcycle=1000)

Cartesian coordinates of the structures

C	-3.01834200	-0.73492900	-0.01503100
C	0.10470700	-1.79334700	-0.00933800
C	-0.46967000	-0.51086100	-0.00601300
C	0.42977300	0.59615100	0.00509900
C	1.82600700	0.52308800	0.00135900
C	2.34430500	-0.78930200	-0.00914100
C	1.48621600	-1.90379100	-0.00154800
H	-0.49742900	-2.69222900	-0.01960100
C	-0.27272300	1.79327200	0.02376200
H	1.94313900	-2.88563400	-0.00135400
C	1.79429700	2.98335700	0.06607200
C	0.40562800	3.01918000	0.05317500
H	2.35492500	3.90976100	0.09667100
H	-0.13466500	3.95861800	0.07021100
C	-1.81802300	-0.00743400	-0.00494600

C	-1.74240000	1.45630000	0.01100500
O	-2.64725400	2.26833900	0.01718200
C	-4.29057200	-0.12068200	-0.01970400
N	-5.36985700	0.30390400	-0.02432500
C	-3.04771300	-2.14350800	-0.02180900
N	-3.08049500	-3.30360400	-0.02766600
N	3.76964200	-1.05862300	-0.02471100
O	4.13988300	-2.15749500	0.35290000
O	4.51776100	-0.17896000	-0.42029500
C	2.50663800	1.77623500	0.04736000
H	3.58711400	1.80029300	0.07088400

S_3 excited state optimization

opt=calcfc freq=noraman td=(nstates=10,root=3,read) PBE1PBE /6-311+g(d,p)scrf=(solvent=acetonitrile,pcm) scf=(tight,maxcycle=1000)

Cartesian coordinates of the structures

C	-3.02772200	-0.75383900	-0.00001500
C	0.10174700	-1.74602200	0.00002100
C	-0.47905500	-0.49749400	0.00000200
C	0.40873500	0.61565300	0.00000300
C	1.84643600	0.55397000	0.00000200
C	2.38188100	-0.77789500	0.00000300
C	1.53391200	-1.85699200	0.00003100
H	-0.47678200	-2.66092300	0.00002600
C	-0.31991400	1.80749700	0.00001600

H	1.97246300	-2.84739300	0.00005500
C	1.78986300	2.96769500	0.00007400
C	0.33932800	2.99958300	0.00004900
H	2.32061300	3.91274800	0.00011400
H	-0.17960600	3.95141100	0.00006400
C	-1.83989800	-0.00447900	-0.00000300
C	-1.78166800	1.45429800	0.00000500
O	-2.70258200	2.25558900	0.00000500
C	-4.31123900	-0.16418100	-0.00001400
N	-5.39839500	0.23969100	-0.00001400
C	-3.02542400	-2.16152800	-0.00003100
N	-3.01820000	-3.32251000	-0.00004400
N	3.80379400	-1.05586200	-0.00003200
O	4.15962800	-2.22222500	0.00035600
O	4.57578800	-0.10987900	-0.00047100
C	2.51581200	1.79603600	0.00005200
H	3.59347300	1.83321600	0.00006700

Table S10. Calculated absorption represented as ΔE in eV, oscillation strengths (f), orbital composition and transition dipole moments (μ) and dipole square (μ^2) of low-lying states of compound **2** (H_0, H_2, H_4, H_5 represent HOMO, HOMO-2, HOMO-4 and HOMO-5 orbitals, respectively. L_0, and L_1 correspond to LUMO, and LUMO-1, respectively. Calculations were performed in acetonitrile using PBE functional and 6-311+g(d,p) basis set.

Excited state	***E* (eV)**	***f***	**composition**	**μ (X, Y, Z)**	**μ^2**
S_1	2.6329	0.1638	H_0-L_0	(1.5937, 0.0075, -0.0000)	2.5400
S_2	2.9683	0.0000	H_2-L_0	(0.0004, 0.0001, 0.0155)	0.0002
S_3	3.3409	0.0743	H_2-L_0 H_0-L_1	(-0.0556, -0.9510, -0.0000)	0.9075
S_4	3.4619	0.4027	H_0-L_1	(2.1751, -0.1291, 0.0000)	4.7476
S_5	3.6553	0.0000	H_5-L_0 H_5-L_1	(-0.0002, -0.0001, -0.0100)	0.0001
S_6	3.8335	0.7906	H_4-L_0	(2.7582, 0.9002, -0.0000)	8.4180

Table S11. Calculated fluorescence represented as ΔE in eV, oscillation strengths (f), orbital composition and transition dipole moments (μ) and dipole square (μ2) of low-lying states of compound **2** (H_0 and H_1 represent HOMO and HOMO-1 orbitals, respectively. L_0 corresponds to LUMO. Calculations were performed in acetonitrile using PBE functional and 6-311+g(d,p) basis set.

Excited state	***E* (eV)**	***f***	**composition**	**μ (X, Y, Z)**	**μ^2**
S_1	2.1447	0.1359	H_0-L_0 (98%)	(1.6041, 0.1138, -0.0020)	2.5860
S_3	2.7919	0.0554	H_1-L_0 (98%)	-0.4983, -0.7496, -0.0000)	0.8101

9.3 Compound **3** Gaussian optimization

Ground state optimization

opt freq=noraman PBE1PBE/6-311+g(d,p) scrf=(solvent=acetonitrile,pcm) geom=connectivity scf=(tight,maxcycle=1000)

Cartesian coordinates of the structures

C	0.53335400	3.01769700	0.00005500
C	-0.13138600	1.81358400	0.00002700
C	0.58652300	0.60844300	0.00000900
C	1.98092400	0.56854700	0.00001800
C	2.65647600	1.81023300	0.00004700
C	1.94382400	2.99560000	0.00006500
H	-0.00352700	3.96014200	0.00006900
C	-0.25182400	-0.54304800	-0.00001900
C	2.57383200	-0.73262000	-0.00000200
H	2.48427200	3.93556600	0.00008700
C	1.76295200	-1.86599800	-0.00003600
C	0.36183200	-1.78383600	-0.00004400
H	2.21662600	-2.84850300	-0.00005900
H	-0.20974900	-2.70415600	-0.00007000
C	-1.56177600	1.45708900	0.00001200
C	-1.61015100	-0.07710500	-0.00001700
C	-2.78892500	-0.76471600	-0.00003100
O	-2.52786700	2.17992000	0.00001800
C	-2.81861500	-2.18589600	-0.00005500
N	-2.84292900	-3.34122400	-0.00007500
C	-4.07103800	-0.14382800	-0.00002500
N	-5.15519300	0.25580600	-0.00002200
H	3.74027900	1.82895300	0.00005500

O	3.90392900	-0.75564900	0.00000800
C	4.57714500	-2.01152300	0.00003800
H	4.32648700	-2.58460700	-0.89641400
H	5.63871500	-1.77475500	0.00009900
H	4.32638700	-2.58461700	0.89645700

S_1 excited state optimization

opt=calcfc freq=noraman td=(nstates=10,root=1,read) PBE1PBE/6-311+g(d,p) scrf=(solvent=acetonitrile,pcm) scf=(tight,maxcycle=1000)

Cartesian coordinates of the structures

C	0.53077200	3.02706400	0.00005300
C	-0.14371700	1.81342900	0.00002700
C	0.60027200	0.62269000	0.00001500
C	1.99741100	0.58204800	0.00002900
C	2.66552700	1.80975200	0.00005400
C	1.92856500	3.00502000	0.00006600
H	-0.00487100	3.96990100	0.00006200
C	-0.24297600	-0.49908600	-0.00001000
C	2.58826400	-0.72657500	0.00001400
H	2.47053300	3.94415900	0.00008600
C	1.74932100	-1.86425000	-0.00001300
C	0.36227800	-1.76485400	-0.00002500
H	2.19519400	-2.85030000	-0.00002500
H	-0.22330100	-2.67567000	-0.00004600
C	-1.58845700	1.45082000	0.00000700
C	-1.63211700	-0.00086100	-0.00001600
C	-2.79212900	-0.77369100	-0.00004000

O	-2.54203000	2.23857300	0.00001000
C	-2.77058700	-2.18500400	-0.00006100
N	-2.77010000	-3.34563300	-0.00007900
C	-4.09379900	-0.21413500	-0.00004600
N	-5.19610000	0.14524600	-0.00005300
H	3.74870100	1.84544300	0.00006600
O	3.89882800	-0.77685700	0.00002800
C	4.57991700	-2.03710500	0.00001700
H	4.32675800	-2.60319000	-0.89846700
H	5.63799600	-1.78973000	0.00003600
H	4.32673300	-2.60321800	0.89847600

S_3 excited state optimization

opt=calcfc freq=noraman td=(nstates=10,root=3,read) PBE1PBE/6-311+g(d,p) scrf=(solvent=acetonitrile,pcm) scf=(tight,maxcycle=1000)

Cartesian coordinates of the structures

C	0.53834000	2.98680800	0.00003400
C	-0.14434800	1.79813300	0.00000900
C	0.58034600	0.61013500	0.00008000
C	2.01358700	0.55935500	0.00009100
C	2.70749200	1.79518700	0.00010200
C	1.99353800	2.96316800	0.00004800
H	0.02424400	3.94191500	0.00010000
C	-0.27957600	-0.51072100	0.00004000
C	2.61052700	-0.73816800	0.00002000
H	2.51564300	3.91265500	0.00005900

C	1.77995300	-1.83619900	-0.00000700
C	0.33185600	-1.73557500	-0.00002200
H	2.20075200	-2.83347300	-0.00000900
H	-0.22746700	-2.66346900	-0.00010200
C	-1.60243800	1.44191200	-0.00002300
C	-1.65590700	-0.00599600	-0.00003100
C	-2.83640100	-0.76791200	-0.00005400
O	-2.53316400	2.25114000	-0.00002100
C	-2.81263700	-2.17488000	0.00000500
N	-2.78776400	-3.33658900	0.00005200
C	-4.12889200	-0.19865600	-0.00011900
N	-5.22422500	0.18490300	-0.00017500
H	3.78966500	1.80476500	0.00012000
O	3.94608100	-0.75934400	0.00001400
C	4.59598500	-2.02565000	-0.00002700
H	4.33356700	-2.59494400	-0.89656000
H	5.66203000	-1.81067300	-0.00003900
H	4.33359700	-2.59498800	0.89648500

Table S12. Calculated absorbance represented as ΔE in eV, oscillation strengths (f), orbital composition and transition dipole moments (μ) and dipole square (μ^2) of low-lying states of compound **3** (H_0, H_1, H_2, and H_3 represent HOMO, HOMO-1 and HOMO-2 orbitals, respectively. L_0 and L_1 correspond to LUMO, and LUMO-1, respectively. Calculations were performed in acetonitrile using PBE functional and 6-311+g(d,p) basis set.

Excited state	***E* (eV)**	***f***	**composition**	**μ (X, Y, Z)**	**μ^2**
S_1	2.3333	0.1979	H_0-L_0	(1.8531, 0.1700, 0.0000)	3.4628
S_2	3.0929	0.0000	H_3-L_0 H_3-L_1	(-0.0000, 0.0000, -0.0103)	0.0001
S_3	3.3799	0.3852	H_0-L_1	(-2.1564, 0.0495, -0.0000)	4.6524
S_4	3.5333	0.0029	H_1-L_0 H_0-L_1	(-0.0653, 0.1714, 0.0000)	0.0336
S_5	3.8570	0.7706	H_2-L_1	(2.7997, 0.5623, 0.0000)	8.1546
S_6	4.3019	0.0129	H_3-L_1	(0.2509, -0.2436, -0.0000)	0.1223

Table S13. Calculated fluorescence represented as ΔE in eV, oscillation strengths (f), orbital composition and transition dipole moments (μ) and dipole square (μ^2) of low-lying states of compound **3** (H_0, and H_1 represent HOMO, and HOMO-1 orbitals, respectively. L_0 corresponds to LUMO. Calculations were performed in acetonitrile using PBE functional and 6-311+g(d,p) basis set.

Excited state	***E* (eV)**	***f***	**composition**	**μ (X, Y, Z)**	**μ^2**
S_1	1.8632	0.1206	H_0-L_0 (98%)	(1.6164, 0.1680, 0.0000)	2.6409
S_3	2.7860	0.0155	H_1-L_0 (99%)	(0.4558, 0.1390, 0.0000)	0.2271

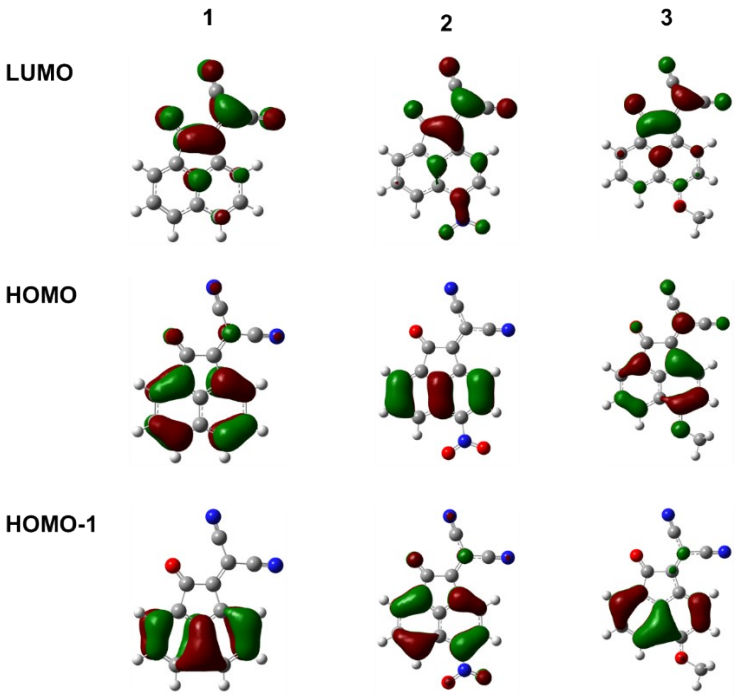

Figure S34. Optimized MOs (NTO) of Compounds **1**, **2**, **3** that involved electronic transitions using PBE functional and 6-311+g(d,p) basis set.

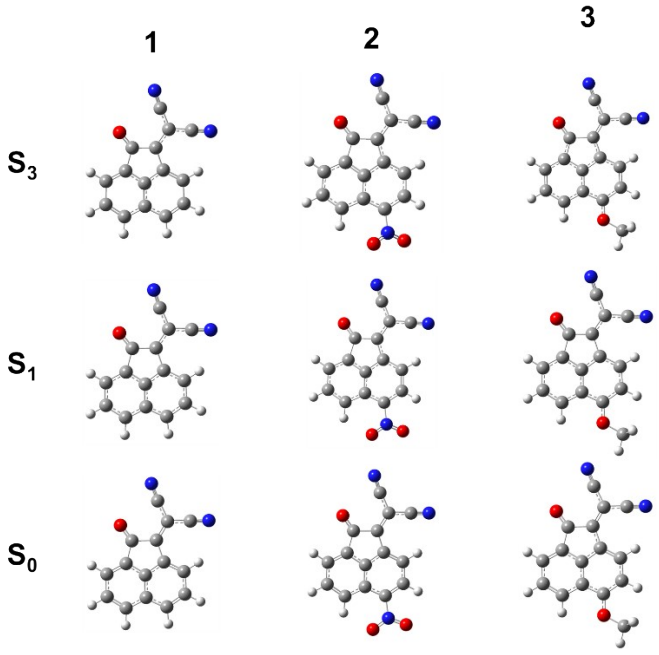

Figure S35. Optimized ground and excited states of Compounds **1**, **2**, **3** using PBE functional and 6-311+g(d,p) basis set.

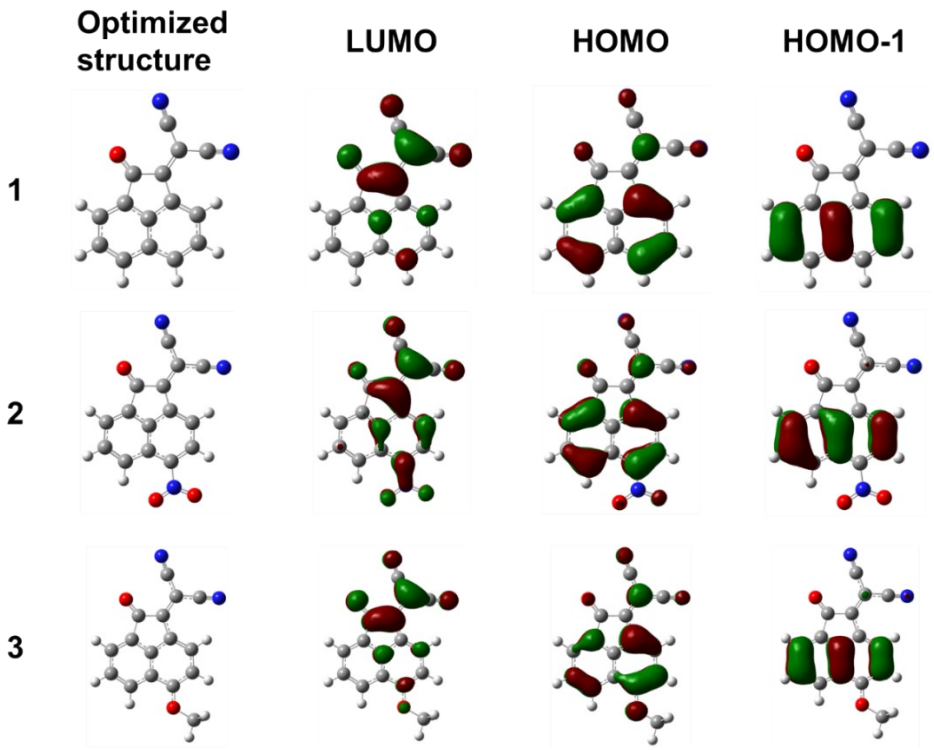

Figure S36. Optimized MOs (NTO) of Compounds **1**, **2**, **3** involved in electronic transitions using cam-b3lyp functional and 6-311g(d,p) basis set.

Table 14. Calculated fluorescence represented as ΔE in eV, oscillation strengths (f), orbital composition and transition dipole moments (μ) and dipole square (μ^2) of low-lying state of compound **1** (H_0, represents HOMO and L_0 corresponds to LUMO. Calculations were performed in acetonitrile using cam-b3lyp functional and 6-311+g(d,p) basis set.

Excited state	***E* (eV)**	***f***	**composition**	**μ (X, Y, Z)**	**μ^2**
S_1	2.4455	0.1855	H_0-L_0 (98%)	(1.7469, 0.2106, -0.0010,)	3.0961

Table 15. Calculated fluorescence represented as ΔE in eV, oscillation strengths (f), orbital composition and transition dipole moments (μ) and dipole square (μ^2) of low-lying state of compound **2** (H_0, represents HOMO and L_0 corresponds to LUMO. Calculations were performed in acetonitrile using cam-b3lyp functional and 6-311+g(d,p) basis set.

Excited state	***E* (eV)**	***f***	**composition**	**μ (X, Y, Z)**	**μ^2**
S_1	2.5243	0.3364	H_0-L_0 (99%)	(2.3130, 0.2987, 0.0001)	5.4392

Table 16. Calculated fluorescence represented as ΔE in eV, oscillation strengths (f), orbital composition and transition dipole moments (μ) and dipole square (μ^2) of low-lying state of compound **3** (H_0, represents HOMO and L_0 corresponds to LUMO. Calculations were performed in acetonitrile using cam-b3lyp functional and 6-311+g(d,p) basis set.

Excited state	***E* (eV)**	***f***	**composition**	**μ (X, Y, Z)**	**μ^2**
S_1	2.2264	0.2407	H_0-L_0 (97%)	(-2.0822, 0.2776, 0.0000)	4.4127

Compound 1 Gaussian optimization

Ground state optimization

opt freq=noraman cam-b3lyp/6-311g(d,p) scrf=(solvent=acetonitrile,pcm)

geom=connectivity scf=(tight,maxcycle=1000)

Cartesian coordinates of the structures

C	-1.06336600	-0.11301000	-0.00004500
C	-0.45632200	-1.52680100	-0.00005900
O	-1.09108500	-2.54828500	-0.00013000
C	1.23851400	0.05297100	0.00006700
C	2.52079900	0.60517100	0.00013700
C	0.04943400	0.82673400	0.00003900

C	0.15687100	2.19702100	0.00008500
H	-0.71113800	2.84126800	0.00006700
C	2.59533700	2.02059400	0.00018300
C	1.44677700	2.77631200	0.00015700
H	1.52488300	3.85597900	0.00019300
H	3.56371500	2.50660300	0.00023700
C	1.00599700	-1.33133800	0.00001100
C	3.59881100	-0.31559800	0.00015000
C	2.05788800	-2.20714100	0.00002400
H	1.90052700	-3.27845400	-0.00001800
C	3.36636800	-1.67237000	0.00009600
H	4.20847900	-2.35260000	0.00010800
H	4.61626400	0.05720800	0.00020400
C	-2.39480200	0.10262500	-0.00010600
C	-2.94135200	1.42287600	-0.00008900
C	-3.36880200	-0.94717400	-0.00020000
N	-4.22597400	-1.71072200	-0.00027700
N	-3.38073500	2.48372700	-0.00007400

First excited state optimization

opt=calcfc freq=noraman td=(nstates=10,root=1,read) cam-b3lyp/6-311+g(d,p) scrf=(solvent=acetonitrile,pcm) scf=(tight,maxcycle=1000)

Cartesian coordinates of the structures

C	-1.05024800	-0.17732700	0.00000000
C	-0.45960900	-1.51801600	0.00003200
O	-1.02831700	-2.59799200	0.00005400
C	1.25656900	0.05458300	0.00001100

C	2.52635200	0.63054100	-0.00001400
C	0.03155500	0.77915700	-0.00002100
C	0.12813000	2.18641300	-0.00009400
H	-0.75297100	2.81165700	-0.00013400
C	2.57999400	2.03550300	-0.00007800
C	1.38625900	2.77500300	-0.00011700
H	1.45136100	3.85526100	-0.00017300
H	3.53289900	2.54998600	-0.00010600
C	1.02657900	-1.30957900	0.00003900
C	3.61705400	-0.26673800	0.00001400
C	2.11291600	-2.18618500	0.00006800
H	1.96337900	-3.25839300	0.00009800
C	3.39777200	-1.64556500	0.00005500
H	4.25138800	-2.30997800	0.00007500
H	4.63023000	0.11583700	0.00000300
C	-2.43019900	0.09052300	0.00000200
C	-2.94250000	1.40419200	0.00014600
C	-3.41109800	-0.92915000	-0.00012000
N	-4.27294300	-1.69678700	-0.00022900
N	-3.36518800	2.47956400	0.00026800

Compound 2 Gaussian optimization

Ground state optimization

opt freq=noraman cam-b3lyp/6-311g(d,p) scrf=(solvent=acetonitrile,pcm)

geom=connectivity scf=(tight,maxcycle=1000)

Cartesian coordinates of the structures

C	-2.97723000	-0.74602200	-0.00001200
C	0.12792200	-1.79202000	-0.00001300
C	-0.43723000	-0.54433300	-0.00001000
C	0.40637800	0.59750600	-0.00000100
C	1.80866900	0.55275400	0.00000400
C	2.33900900	-0.77328900	-0.00000100
C	1.53235200	-1.88312200	-0.00000700
H	-0.45658600	-2.69996400	-0.00001900
C	-0.31781700	1.80256200	0.00000500
H	2.00265400	-2.85500700	-0.00000600
C	1.73804800	2.98553700	0.00002600
C	0.32914800	3.00584300	0.00001900
H	2.27533400	3.92524800	0.00003700
H	-0.21520500	3.94149700	0.00002300
C	-1.81785400	-0.06305700	-0.00000800
C	-1.75386000	1.46623400	-0.00000900
O	-2.70616700	2.19939100	0.00000700
C	-4.26383100	-0.11480000	-0.00001300
N	-5.33647200	0.29270500	-0.00001400
C	-3.01528600	-2.17529700	-0.00001700
N	-3.04792500	-3.32257900	-0.00002000
N	3.79089200	-1.03227400	-0.00000200
O	4.16685800	-2.18770000	0.00015300
O	4.54537100	-0.07820000	-0.00012000
C	2.46194400	1.81449000	0.00001800
H	3.53767500	1.85741200	0.00002400

First excited state optimization

opt=calcfc freq=noraman td=(nstates=10,root=1,read) cam-b3lyp/6-311+g(d,p) scrf=(solvent=acetonitrile,pcm) scf=(tight,maxcycle=1000)

Cartesian coordinates of the structures

C	-3.01357200	-0.74276200	0.01744900
C	0.10827700	-1.79825900	0.05491900
C	-0.47700500	-0.51159500	0.02580100
C	0.42399400	0.60651700	-0.00706200
C	1.82062000	0.53355500	-0.00781900
C	2.33575600	-0.77960100	0.01989600
C	1.48033100	-1.90120800	0.03706900
H	-0.49180600	-2.69529000	0.09073200
C	-0.27455900	1.79504600	-0.03455800
H	1.94533300	-2.87607400	0.04482200
C	1.79071700	2.98200000	-0.11650000
C	0.40165200	3.01513800	-0.09501200
H	2.34600600	3.90852000	-0.16820800
H	-0.13885400	3.95220100	-0.12825200
C	-1.81098900	-0.02406600	0.01614900
C	-1.73726800	1.45836300	-0.00776500
O	-2.64940200	2.25063500	-0.01966900
C	-4.28219000	-0.11709600	0.05773400
N	-5.34992900	0.31776300	0.09113700
C	-3.04299700	-2.15313800	-0.02554900
N	-3.06522700	-3.30667900	-0.05969800
N	3.76251200	-1.05293900	0.03821600

O	4.14798900	-2.08669500	-0.48351300
O	4.50087000	-0.24744600	0.58493400
C	2.49971400	1.78217100	-0.08011300
H	3.57729100	1.80129800	-0.10852000

Compound 3 Gaussian optimization

Ground state optimization

opt freq=noraman cam-b3lyp/6-311g(d,p) scrf=(solvent=acetonitrile,pcm)

geom=connectivity scf=(tight,maxcycle=1000)

Cartesian coordinates of the structures

C	2.78651100	-0.76948000	0.00008400
C	-0.36420700	-1.78074200	-0.00008500
C	0.25014300	-0.54778700	-0.00014100
C	-0.58239600	0.60538900	-0.00015900
C	-1.97239900	0.56901900	-0.00006300
C	-2.57079200	-0.72978000	-0.00003700
C	-1.76849100	-1.86101200	-0.00005600
H	0.20328400	-2.70121300	-0.00004900
C	0.13589200	1.80934000	-0.00020000
C	-2.64615200	1.81200500	0.00002400
H	-2.22186800	-2.84111100	-0.00001600
C	-1.93490900	2.99219400	0.00004900
C	-0.52343400	3.01003900	-0.00004700
H	-3.72800900	1.82877600	0.00010700
H	-2.47133300	3.93232200	0.00013100
H	0.01590400	3.94913200	-0.00007100
C	1.61874300	-0.08452700	-0.00009400

C	1.56956200	1.45493800	-0.00048600
O	2.53181500	2.17610000	0.00006400
C	4.07381800	-0.14696000	0.00002400
N	5.14894600	0.25705600	-0.00003800
C	2.80980900	-2.19620100	0.00031800
N	2.82146300	-3.34504600	0.00052100
O	-3.90498600	-0.74209800	0.00003100
C	-4.59202100	-1.99316400	0.00010200
H	-4.34685800	-2.56832000	0.89480200
H	-5.64968500	-1.74693800	0.00017900
H	-4.34699400	-2.56834700	-0.89461900

First excited state optimization

opt=calcfc freq=noraman td=(nstates=10,root=1,read) cam-b3lyp/6-311+g(d,p) scrf=(solvent=acetonitrile,pcm) scf=(tight,maxcycle=1000)

Cartesian coordinates of the structures

C	2.79874500	-0.77828500	0.00001100
C	-0.35585400	-1.76788000	0.00005600
C	0.25828800	-0.49806800	0.00001600
C	-0.60020700	0.62683300	-0.00001500
C	-1.99023800	0.58219900	-0.00001100
C	-2.57780700	-0.72724000	0.00002900
C	-1.73510200	-1.86570700	0.00006200
H	0.23019700	-2.67593100	0.00008200
C	0.13300200	1.81270500	-0.00005000
C	-2.66518900	1.80714800	-0.00004500
H	-2.18114100	-2.84915400	0.00009200

C	-1.93921600	3.00120600	-0.00008000
C	-0.54321300	3.02325100	-0.00008400
H	-3.74681500	1.83193600	-0.00004300
H	-2.48166700	3.93765700	-0.00010600
H	-0.00671500	3.96378100	-0.00011300
C	1.62713800	-0.01002800	-0.00000300
C	1.58054600	1.45053300	-0.00004400
O	2.52492600	2.23455600	-0.00006500
C	4.09374100	-0.20409800	0.00000300
N	5.18286300	0.17702300	-0.00000100
C	2.77837300	-2.18932300	0.00003700
N	2.76526800	-3.34470000	0.00005700
O	-3.88510400	-0.78040000	0.00003400
C	-4.57716400	-2.04152100	0.00007000
H	-4.32654000	-2.60599100	0.89767900
H	-5.63132900	-1.78610900	0.00006300
H	-4.32654000	-2.60604300	-0.89750700

Reference

i L. Wanga, X. Wanga, J. Cuia, W. Rena, N. Menga, J. Wanga and X. Qian, *Tetrahedron:Asymmetry*, 2010, **21,** 825–830